International Journal of Biological Macromolecules 151 (2020) 529–544

Contents lists available at ScienceDirect

International Journal of Biological Macromolecules

journal homepage: http://www.elsevier.com/locate/ijbiomac

Phylogeography of the cicada *Platypleura hilpa* in subtropical and tropical East Asia based on mitochondrial and nuclear genes and microsatellite markers

Yunxiang Liu [a], Hong Thai Pham [b], Zhiqiang He [c], Cong Wei [a,*]

[a] State Key Laboratory of Crop Stress Biology for Arid Areas, Key Laboratory of Plant Protection Resources and Pest Management, Ministry of Education, College of Plant Protection, Northwest A&F University, Yangling, Shaanxi 712100, China
[b] Vietnam National Museum of Nature Vietnam Academy of Science and Technology, 18 Hoang Quoc Viet Street, Cau Giay, Hanoi, Viet Nam
[c] College of Plant Science, Tarim University, Alar, Xinjiang 843300, China

ARTICLE INFO

Article history:
Received 8 January 2020
Received in revised form 16 February 2020
Accepted 16 February 2020
Available online 19 February 2020

Keywords:
Ancestral area reconstructions
Climate oscillations
Dispersal
Evolutionary history
Hemiptera
Genetic differentiation

ABSTRACT

Climate change and geographical events play key roles in driving population genetic structure of organisms, but different scenarios were suggested for species occurring in tropical and subtropical areas. We investigated the population genetic structure, diversity and demographic history of the cicada *Platypleura hilpa* which occurs in coastal areas of southern China and northeastern Indo-Burma, and analysed the potential impact of climate change and geological events on its evolutionary history. Our data imply that *P. hilpa* comprises five main lineages with nearly unique sets of haplotypes and distinct geographic distributions. A major split of the lineages occurred in the Pleistocene. Geographic distance and geomorphic barriers serve as the primary factors shaping the genetic population structure, and several climatic factors are associated with the divergence. The potential range during the Last Glacial Maximum has apparently increased in south China and the exposed South China Sea Shelf. The Pleistocene sea-level fluctuations had profound effects on the regional genetic structure. The Beibu Gulf represents a more important geographic barrier than the Qiongzhou Strait in blocking gene flow among populations. These results contribute to a better understanding of the pressure climatic change and geographical events impose on insects in coastal areas of East Asia.

1. Introduction

The origin and evolution of biodiversity, essentially speciation, has been associated with sexual selection, behavioral change, disruptive ecological selection and disruption of gene flow [1,2]. The past and present distributions of invertebrate species are strongly linked to climate, e.g., the Pleistocene glaciations especially in temperate latitudes [3,4]. The tropical and subtropical areas have never been covered by ice sheets [5,6], where invertebrates exhibit a wide local diversity and seem to have developed a much stronger bond with the ecosystem than their temperate counterparts [6,7]. Combined with local geological events, climatic oscillations are an important evolutionary driver, having a deep impact on shaping the structure of biotas [8]. Climatic fluctuations during the Pleistocene are responsible for the isolation of populations in multiple refugia [9,10]. Due to isolation in small refugia, bottlenecking, founder effects and genetic drift contribute to lower genetic diversity and population divergence [11,12]. In these refugia, persistence of stable microclimates facilitates survival during periods of intense fluctuations. Species then generally shift to more favourable habitats or undergo successful evolutionary adaptations [13]. In addition, geological changes, such as the separation of formerly adjacent land masses, result in range fragmentation which can form barriers to gene flow and lead to genetic diversification and speciation [14–16]. Sometimes, climatic fluctuations and geological changes work together as co-drivers, leading to genetic diversification and speciation [17,18]. These relative roles that climate and geography play in driving genetic patterns have important implications for diversification, conservation, and biogeography [19].

During the past three million years, global climate has fluctuated greatly [5]. The recent major ice age and sea-level fluctuations have led to substantial changes in the distribution of many living organisms, especially taxa in temperate zones [2,6,20]. During the Pleistocene, glacial and interglacial climatic shifts resulted in sea-level changes with amplitudes of up to 120–140 m, with cyclic formation and submergence of land bridges between landmasses including subtropical and tropical zones [21]. These changes repeatedly dissected and rejoined populations of many species, and produced intermittent range contractions and expansions. Island populations isolated from their mainland relatives could then drive allopatric divergence and incipient speciation. In addition, significant geological events, such as the formation of

* Corresponding author.
E-mail address: congwei@nwsuaf.edu.cn (C. Wei).

https://doi.org/10.1016/j.ijbiomac.2020.02.183
0141-8130/

mountain ranges, also were a source of long-term biogeographical barriers [22]. It is reasonable to assume that climate-mediated changes in sea level and the formation of mountain ranges likely contributed to genetic variation and divergence among populations and species occurring in related areas.

Paleogeographic reconstructions of fauna provide guidance for formulating testable phylogeographic hypotheses, as well as a detailed picture of population history [23]. The distributional dynamics through time are expected to have genetic consequences. Ecological niche modelling (ENM) can be used to infer past species distributions, which may supplement the shortage of fossil records in related regions. ENMs have the potential to show how habitat quality affects genetic diversity and genetic connectivity. Together with molecular data, we can better understand the population dynamics over time and evaluate the habitat suitability across a certain range [24]. Nevertheless, the prominent role of older environmental shifts, such as climate-mediated changes in sea level and the formation of mountain ranges, in the evolution and/or differentiation of modern insects have rarely been studied.

Many studies have concluded that temperate species populations contracted in glacial refugia during the cold stages, following a geographical expansion during the interglacial phases [20,25]. However, different scenarios have been suggested for species occurring in tropical and subtropical areas, because these regions were never covered by ice sheets, although they did experience cooler and drier climates within the Miocene [5,6,26]. One such example is Hainan Island on the northeastern margin of the Indo-Burma region, one of the most severely protected biodiversity hotspots in the world, which has experienced connection-disconnection events with the Chinese mainland due to sea-level fluctuations throughout the Pleistocene [27]. The topologically complex coastal areas of the Indo-Burma region including southern China are an important biodiversity hotspot in East Asia [28], providing an excellent study system for detecting the relative contributions of paleogeographic processes to local species richness. Hainan Island is located in the transitional zone between the subtropical and tropical zones in the South China Sea, which is adjacent to the coastal areas of southern China and northern Vietnam. This region is a globally important biodiversity hotspot, harbouring high levels of endemism and species richness [28]. Phylogenetic methods and ENMs have been applied to study some of the fauna in Hainan Island [14,29]. While most previous studies used genetic discontinuities to demonstrate the phylogeography of endemism in Hainan Island, ecological data were not explicitly examined to support those processes. How the dispersal and vicariance scenarios in Hainan and the adjacent mainland regions due to landscape alterations remains poorly explained.

Cicadas are excellent subjects for bio-geographical studies because of their low dispersal ability caused by their generally long, subterranean pre-adult stage and short adult lifespan compared with other insects [30,31]. Recent phylogeographical studies have been conducted with cicadas as model organisms in New Zealand [32], the Iberian region [33], and East Asia [34]. The cicada *Platypleura hilpa* Walker is patchily distributed primarily in coastal areas of southern China and northern Vietnam, and on various islands in the South China Sea, but it has not been found in the inland of China south to Changjiang (Yangtze) River (Fig. 1). Osozawa et al. [35] used *P. hilpa* as the outgroup to reconstruct the phylogenetic trees of several other *Platypleura* species collected primarily from the Japan–Ryukyu–Taiwan islands, including specimens collected from continental Korea–China. However, population differentiation and phylogeography of this species have never been investigated. Here we use an integrative approach, combining genetic data with climatic and paleoenvironmental data, to elucidate the demographic history and phylogeography of *P. hilpa*. Our specific objectives were, to unravel the phylogeography of *P. hilpa* and to determine in detail the main ecological factors which affect the population genetic structure and evolutionary history of this species. The outcome of these analyses will contribute to a better understanding the effects that climatic changes and geographic isolation impose on insects occurring in subtropical and tropical coastal areas of East Asia.

2. Results

2.1. Diversity indices and neutrality test

For the combined mitochondrial genes (*COI* + *COII* + *Cytb*), we observed 96 haplotypes among the 28 populations (except for the population from Babuyan Island) (Table S1). This high haplotype diversity among genes ranged from 0.152 to 1.000; the haplotype diversity (h) among populations varied from 0.152 (XM) to 1.000 (LJ); and the nucleotide diversity (π) ranged from 0.00046 (TGL and DX) to 0.01077 (SX) (Table 1). Overall, the mean haplotype diversity was higher in populations from Hainan Island (0.963) than from the China mainland (0.914) and northern Vietnam (0.436), but the nucleotide diversity in populations from Hainan Island (0.00477) was lower than for the mainland populations (0.00826). Populations of *P. hilpa* from both Hainan Island and the China mainland have a high level of genetic diversity. Neutrality tests conducted for the combined mtDNA dataset of the 28 populations (again except for the Babuyan Island population) (Table 1) indicate that the Tajima's D was not significantly different in all of the populations analysed.

The pairwise Fst ranged from −0.027 (BWL and ZH populations) to 0.487 (TGL and YJ populations) (Table S2). Significantly, genetic divergence was found between the HA population and the remaining populations, with the maximum mean differentiation value (mean Fst ¼ 0.235) varying from 0.096 to 0.312. The Mantel test results produced an r value of 0.297 and 0.19 for combined mitochondrial gene data ($p = .0019$; $p = .015$) (Fig. S1), indicating a significant correlation between the genetic distance and the geographic distance in *P. hilpa* populations.

2.2. Phylogenetic and genetic structure

We used *COI* and concatenated (*COI* + *18S*) genes to construct phylogenetic trees of all the sampled populations of *P. hilpa* and the outgroup species, respectively (Fig. 2). Seventy-seven haplotypes of *COI* gene and 107 haplotypes of concatenated (*COI* + *18S*) genes were identified (Table S1). The results of both ML and BI trees based on the *COI* gene separate *P. hilpa* populations into five major clades and five haplogroups, i.e., Clade A (Babuyan Island, BBY), Clade B (southeast China, SEC), Clade C (Clades C1–C4, Hainan Island, HN), Clade D (Clades D1–D4, south China, SC), and Clade E (northern Vietnam, NV) (Fig. 2a). It is the same that the results of BI tree based on concatenated genes (*COI* + *18S*) separate *P. hilpa* populations into five major clades and five haplogroups, i.e., Clades A–E (Fig. 2b). Accordingly, five clades (Clades A–E) are found in the network based on the *COI* gene (Fig. 3). The results based on the *COI* gene indicate that Clades C2 and D3 are not monophyletic, but the network demonstrated they are individual clade (Figs. 2a, 3). The genetic variation among the haplogroups is 71.43% (AMOVA, $K = 5$, Table 2). In addition, four subclades (Clades C1–C4) are found in the network based on mtDNA (*COI* + *COII* + *Cytb*) for the Hainan Island populations (Fig. 1b).

We further used concatenated mitochondrial genes (*COI* + *COII* + *Cytb*) to analyse the population structure of all the populations from the China mainland, Hainan Island and Vietnam. The ML analysis is consistent with the Bayesian topology (Fig. S2). The results of both ML and BI trees separate *P. hilpa* populations into four major clades and four haplogroups, i.e., Clade B, Clade C, Clade D and Clade E. Similarly, the haplotype network of mtDNA data (Fig. S2c) also presents four clusters corresponding to these four clades.

Results from the AMOVA ($K = 4$) for the populations from the China mainland, Hainan Island and Vietnam show that the overall genetic variation among the four haplogroups is 82.13%, whereas it is only 15.11% among populations within haplogroups, and 2.76% within populations

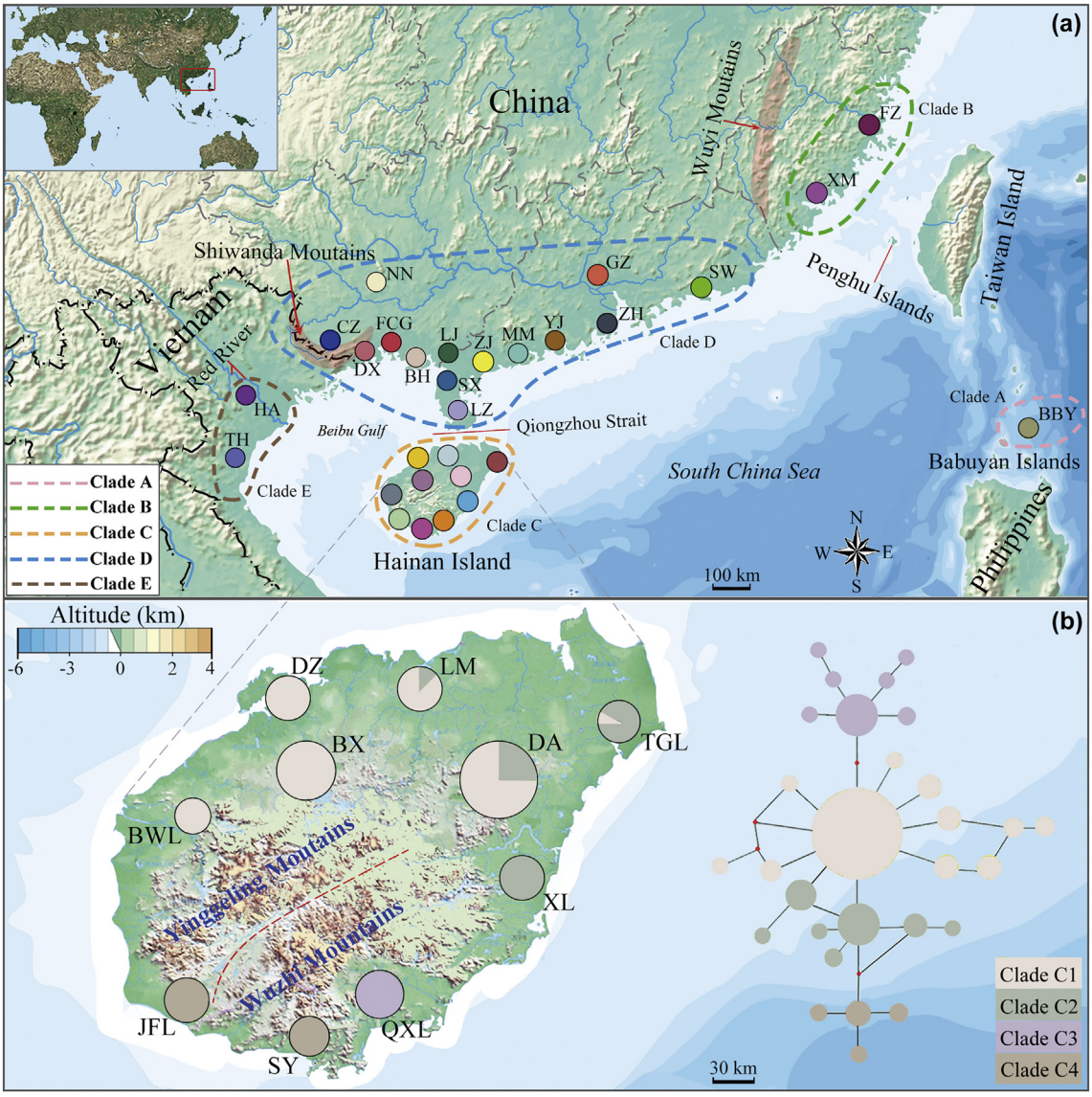

Fig. 1. Geographic distribution of *P. hilpa*. (a) Distribution of *P. hilpa*. (b) Geographic distribution of the mtDNA haplotypes detected in the Hainan Island. Coloured dots represent sampling sites. Dashed colour areas represent different Clade and are the same as in Fig. 2. Detailed information on the locations and codes for the populations are presented in Table 1. (For interpretation of the references to colour in this figure legend, the reader is referred to the online version of this chapter.)

(Table 2). The fixation index is high and statistically significant. The AMOVA results show that most of the genetic variation is attributed to differences among haplogroups.

We also constructed phylogenetic trees for all the *P. hilpa* populations except for the Babuyan Island population based on concatenated mitochondrial and nuclear genes (*COI* + *COII* + *Cytb* + *EF-1α* + *18S* + *ITS1*) (Fig. S3). Both the ML and BI analyses indicate a similar topology (Fig. S3). The topological structures based on both joint mitochondrial genes and nuclear genes are consistent with the corresponding network, and are roughly the same with trees constructed using concatenated mitochondrial genes as well as individual nuDNA (Figs. 4a, S2, S3).

2.3. Population structure based on microsatellite data

In the Bayesian analysis of population structure (Fig. 4b), the highest likelihood of the SSR data was obtained when samples were clustered into four groups (K = 4). The first group was composed of samples from 10 populations in Hainan Island; the second group comprised samples of the two populations from northern Vietnam; the third group consisted of samples from the 14 populations from south China; and the fourth group comprised samples of the two populations from southeast China. Generally, most individuals in each population were assigned to a particular group, but the LM and TGL populations of northern Hainan Island comprised a mixture of individuals belonging to the first and third groups (Fig. 3b). Subsequent hierarchical analyses of individuals of upper groups show a helispherical population structure with K value increasing, until K = 7 without any trace of stable differentiation (Fig. 3b). Thus, a total of four geographical subgroups were found for the populations from the China mainland and Hainan Island. Results produced by STRUCTURE analyses are very similar to those of the network analyses (Figs. 3, 4, S2).

2.4. Genetic distances (K2P)

The number of mitochondrial haplotypes within haplogroups (Clades B–E) ranges from eight (Clade E) to 51 (Clade C) (Table S3). The haplotype diversity is large, ranging from 0.401 (Clade E) to 1 (Clades C and D). The nucleotide diversity ranges from 0.00047 (Clade E) to 0.00625 (Clade D). The pairwise corrected genetic distances

Table 1
Samples, genetic diversity and the demographic analysis of 28 populations of *P. hilpa* based on the mtDNA genes.

Collecting locality	Locality code	Sample size	Longitude, latitude	Collection date	S	*h*	P	*π* (%)	D(p)	*τ*	Fu's Fs	SSD
Bawangling	BWL	10	109°03′ E 19°07′ N	28 May2014	3	0.457	6.161	0.425	−1.26022 (0.0950)	8.36111	-2.756^{NS}	0.042^{NS}
Bangxi	BX	12	109°06′ E 19°22′ N	1 Jun 2014	6	0.675	3.152	0.250	−1.22601 (0.8890)	9.80555	-6.062^{NS}	0.797^{NS}
Dingan	DA	14	110°21′ E 19°40′ N	4 Jun 2014	10	0.857	5.169	0.197	−1.4611 (0.0530)	20.31654	-3.068^{**}	0.202^{NS}
Danzhou	DZ	10	109°34′ E 19°30′ N	1 Jun 2014	3	0.364	3.444	0.425	−0.52775 (0.3350)	9.06161	-2.742^{NS}	0.697^{NS}
Jianfengling	JFL	12	109°01′ E 18°40′ N	26 Aug 2014	7	0.633	2.344	0.094	−0.47371 (0.0580)	0.66498	-0.369^{NS}	0.074^{NS}
Leiming	LM	10	110°19′ E 19°33′ N	3 Jun 2014	4	0.500	5.789	0.159	0.29513 (0.4630)	30.12645	0.102^{NS}	0.032^{NS}
Qixianling	QXL	10	109°41′ E 18°41′ N	14 May 2014	8	0.867	17.632	0.177	0.49570 (0.3490)	0.31686	10.57^{NS}	0.797^{NS}
Sanya	SY	8	108°57′ E 18°11′ N	30 May 2014	5	0.733	2.546	0.074	−1.37471 (0.0690)	0.77894	-0.693^{NS}	0.047^{NS}
Tongguling	TGL	14	111°01′ E 19°40′ N	26 Aug 2014	5	0.524	2.131	0.046	0.78976 (0.8430)	3.65874	1.247^{NS}	0.063^{NS}
Xinglong	XL	12	110°12′ E 18°45′ N	29 May 2014	6	0.800	12.364	0.128	−0.43010 (0.3970)	0.96587	-1.57^{NS}	0.151^{*}
Beihai	BH	20	108°50′ E 21°29′ N	23 May 2016	5	0.942	8.369	0.506	−1.28787 (0.0731)	8.46753	-0.415^{NS}	0.306^{NS}
Chongzuo	CZ	10	107°50′ E 22°20′ N	19 May 2016	2	0.157	8.169	0.431	−1.37033 (0.0720)	0.64897	-2.973^{NS}	0.052^{NS}
Dongxing	DX	10	105°04′ E 29°59′ N	18 May 2016	2	0.300	7.189	0.046	−1.01308 (0.1630)	9.34678	-0.359^{NS}	0.043^{NS}
Fangcheng	FCG	20	108°02′ E 21°45′ N	17 May 2016	6	0.846	9.556	0.46	0.62482 (0.2980)	8.79465	3.213^{*}	0.221^{NS}
Fuzhou	FZ	8	119°29′ E 26°07′ N	1 Jun 2017	2	0.252	4.461	0.178	1.66370 (0.3172)	7.49852	-1.575^{*}	0.121^{NS}
Guangzhou	GZ	24	110°23′ E 21°12′ N	20 Jun 2017	3	0.560	4.254	0.188	−1.10628 (0.2291)	7.54635	-9.347^{NS}	0.758^{*}
Leizhou	LZ	20	110°05′ E 20°54′ N	1 Jun 2016	10	1.000	7.125	1.063	−1.46110 (0.0530)	0.36452	-1.376^{NS}	0.076^{NS}
Lianjiang	LJ	10	110°18′ E 21°36′ N	6 Jun 2014	7	0.866	9.126	0.055	−1.18678 (0.1010)	8.46797	-2.188^{NS}	0.68^{NS}
Maoming	MM	20	110°21′ E 21°34′ N	6 Jun 2016	4	0.722	4.125	0.131	−1.29261 (0.0690)	11.45531	-9.327^{NS}	0.003^{NS}
Nanning	NN	5	108°33′ E 22°54′ N	21 May 2016	3	0.36	3.2154	0.098	1.10628 (0.1290)	6.64335	-8.447^{NS}	0.658^{*}
Sanwei	SW	9	115°21′ E 23°08′ N	21 May 2016	2	0.751	8.564	1.077	0.78976 (0.1400)	6.36154	0.477^{NS}	0.124^{NS}
Suixi	SX	20	110°14′ E 21°22′ N	6 Jun 2014	7	0.833	2.564	0.071	0.45976 (0.1100)	3.10051	0.727^{NS}	0.380^{NS}
Xiamen	XM	5	118°08′ E 24°48′ N	28 May 2017	2	0.152	6461	0.228	0.66370 (0.2451)	6.49852	-2.575^{*}	0.321^{NS}
Yangjiang	YJ	20	111°21′ E 22°41′ N	8 Jun 2015	5	0.886	3.684	0.121	−0.42693 (0.4501)	8.79023	−4.365	0.062^{NS}
Zhanjiang	ZJ	20	110°′03 E 21°02′ N	4 Jun 2015	7	0.739	4.369	0.101	−0.42693 (0.18302)	10.36457	-4.210^{**}	0.052^{*}
Zhuhai	ZH	20	113°03′ E 22°27′ N	9 Jun 2015	8	0.901	6.238	0.18	−0.69176 (0.7530)	10.43277	-2.039^{NS}	0.003^{NS}
Hanoi	HA	8	113°17′ E 23°8′ N	20 Jun 2013	6	0.485	3.684	0.121	−0.42693 (0.1515)	8.79023	−4.365	0.062^{NS}
Thanh Hoá	TH	4	105°48′ E 19°56′ N	14 Jun 2013	3	0.386	4.185	0.331	−0.35691 (0.01245)	6.59032	−5.551	0.112^{NS}
Babuyan island	BBY	4	121°27′ E 19°18′ N	GeneBank data	2	–	–	–	–	–	–	–

Number of haplotypes (S), haplotype diversity (*h*), nucleotide diversity (*π*), average number of pairwise differences (P) in populations of *P. hilpa* from different regions, Tajima's D (p) and expansion (coalescence) time under the sudden expansion assumption in mutation generations (*τ*), Fu's Fs, sum of square deviation (SSD), NS, not significant. Superscript denotes Region.
* 0.05 ≥ p ≥ 0.01.
** 0.01 > p ≥ 0.001.

based on *COI* sequences of *P. hilpa* and other *Platypleura* species are shown in Table S3. Intraspecific genetic distances of *P. hilpa* (0.000–0.049) are distinctly lower than those between *Platypleura* species (0.088–0.157), without overlap. This indicates that the variations of populations of *P. hilpa* have not reached species level. The intraspecific genetic distances between Babuyan clade (Clade A) and Clade D (populations of Hainan Island) are the highest (Table S4).

2.5. Estimation of divergence time

The BEAST-derived combined *COI* and *18SrRNA* gene chronogram of *P. hilpa* recovered 107 haplotypes (H1–107). The chronogram was calibrated by setting the date of the MRCA of *P. hilpa* at 1.55 ± 0.15 Mya (node 2 in Fig. 5a). Our results suggest that all populations of *P. hilpa* began to diversify in the Pleistocene around 1.55 ± 0.15 million years ago (Ma) (node 2 in Fig. 5a), with the subsequent establishment of four clades (Clades B–E) during the Pleistocene (nodes 2–4 in Fig. 5a). The divergence time between Clade B and Clade C + D + E is estimated to be 1.32 Ma in the early Pleistocene (95% HPD: 0.90–1.74 Ma) (node 3 in Fig. 5a). The divergence of Clade C and Clade D + E occurred in the early Pleistocene at 1.08 Ma (95% HPD: 0.76–1.40 Ma) (node 4 in Fig. 5b), and the divergence of Clade D and Clade E occurred in the middle Pleistocene at 0.88 Ma (95% HPD: 0.57–1.19 Ma) (node 5 in Fig. 5a). The estimated divergence time obtained from the *BEAST analysis is on average slightly older than that based on the concatenated mitochondrial haplotypes (Fig. 5b).

2.6. Demographic history

Neutrality tests were conducted for each of the four haplogroups (Clades B–E) of *P. hilpa* (except for the Babuyan Island population) with the combined mtDNA dataset (Table S3). Mismatch distribution analyses reveal a multimodal distribution for these haplogroups (Fig. 6). Among the four haplogroups, Clade C (HN) and Clade D (SC) show significant, negative values for both Fu's Fs (p < .01) and Tajima's D (p < .01) tests (Table S3), rejecting a neutral evolution hypothesis and indicating that recent population expansion has occurred within these two lineages. The unimodal curves found with the mismatch distribution provide the same inference of the neutrality tests (Fig. 6), i.e., two haplogroup expansions have occurred (i.e., Clades C and D) (Fig. 6b, c). The effective population size estimated for each haplogroup reveals different profiles of historical demography. The population size of the SEC (Clade B) and NV (Clade E) remains stable. The minor lineages of Clade E exhibit a slight decrease in population size, corresponding to their limited distribution in two sampling sites in Vietnam (HA and TH). The major lineage of Clade C shows a slight expansion of population size at ~0.68 Ma (Fig. 6b). The obvious increase in population size found in the recently derived haplogroup of Clade D, at ~0.021 Ma (LGM) (Fig. 6c), demonstrates a demographic and range expansion, which is also supported by the mismatch distribution analysis. The star-like structures of the haplotype network corroborates these results (Figs. 3, S2c).

2.7. Ancestral area reconstruction and diversification analysis

Based on the topology of the intraspecific chronogram (Fig. 5a), the BBM analysis of ancestral distribution areas (Fig. 7b) supports a possible ancient (pre-Quaternary) distribution of *P. hilpa* in southeast China (A in Fig. 7a, b) and south China as well as potentially northeast Vietnam (node I in Fig. 7b, B in Fig. 7), which was likely followed by independent colonizations from south China (node II in Fig. 7b) to partial region of north Vietnam (D in Fig. 7), and then to Hainan Island (C in Fig. 7). The likely origin of *P. hilpa* was in one of the A or B regions, but the precise ancestral area was not revealed. The LTT plots indicate that the southeast China and south China groups exhibit a relatively slow and almost constant rate of lineage accumulation. The completely

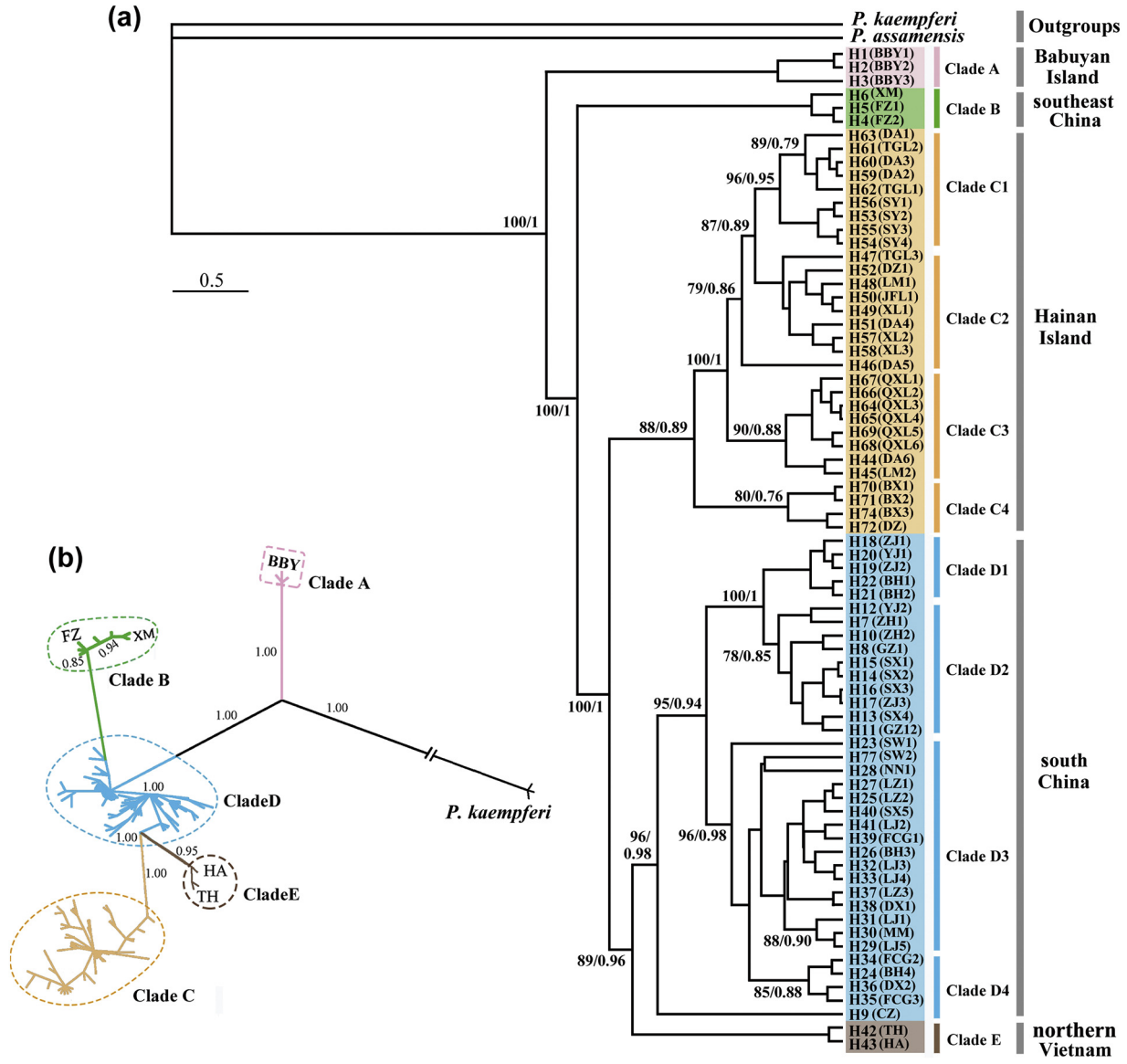

Fig. 2. Phylogenetic tree. (a) Phylogram reconstructed based *COI* gene, nodal values near branches indicate bootstrap supports and posterior probabilities of ML/BI, constructed using BEAST and drawn by FigTree. (b) Bayesian phylogram estimated from concatenated (*COI* + *18S*) genes, constructed using MRBAYES and drawn by FigTree. Numbers at the nodes are posterior probabilities.

reconstructed LTT for *P. hilpa* shows a roughly constant diversification rate during the Pleistocene at around 2.0 Ma (Fig. 7c).

2.8. Present and past ecological niche models

The AUC value for the present potential distribution of *P. hilpa* is high (0.858 ± 0.017), indicating a good model fit. The predicted distribution of this species under present conditions (1950–2000) (as shown in Fig. 8a) is generally similar to its actual distribution on the China mainland, Hainan Island, northern Vietnam and Babuyan Island, with a potentially continuous range in south China and a more patchy one alongside the coastline of southeast China. The potential distribution range during the LGM contracted greatly in its southeast part, especially alongside the coastline of southeast China (Fig. 8b). In contrast, the potential distribution during the LGM was apparently increased in south China, and remained more or less stable in the Leizhou Peninsula and expanded on the exposed South China Sea Shelf (including present-day Hainan Island) (Fig. 8b). Despite a southwestward range shift in general, this species did not retreat entirely to the tropical south during the LGM (Fig. 8b).

3. Discussion

Correctly evaluating the population differentiation and the phylogenetic relationships among populations of the cicada *P. hilpa* had been a challenging endeavor, but intraspecific relationships for different lineages of *P. hilpa* are clear. In addition to a mtDNA phylogeny, we now have a complementary, well supported nuDNA phylogeny, with which we can assess the differentiation of *P. hilpa* and gain further insight into the evolution and phylogeography of this species. Our analysis of molecular data suggests that *P. hilpa* is composed of five main lineages (Clades A–E) with almost unique sets of haplotypes and distinct geographic distributions in, respectively, Babuyan Island, Hainan Island, and the adjacent mainland (Figs. 2–4, S2). In conjunction with our molecular dating (Fig. 5), the ancestral range reconstructions (Fig. 7) indicate that a major split (Clades A–E) occurred in the Pleistocene, which provides insights into revealing the potential impact of climate change on this herbivorous insect and other terrestrial organisms in subtropical and tropical coastal areas of southern China, the northeastern margin of the Indo-Burma region, and adjacent islands.

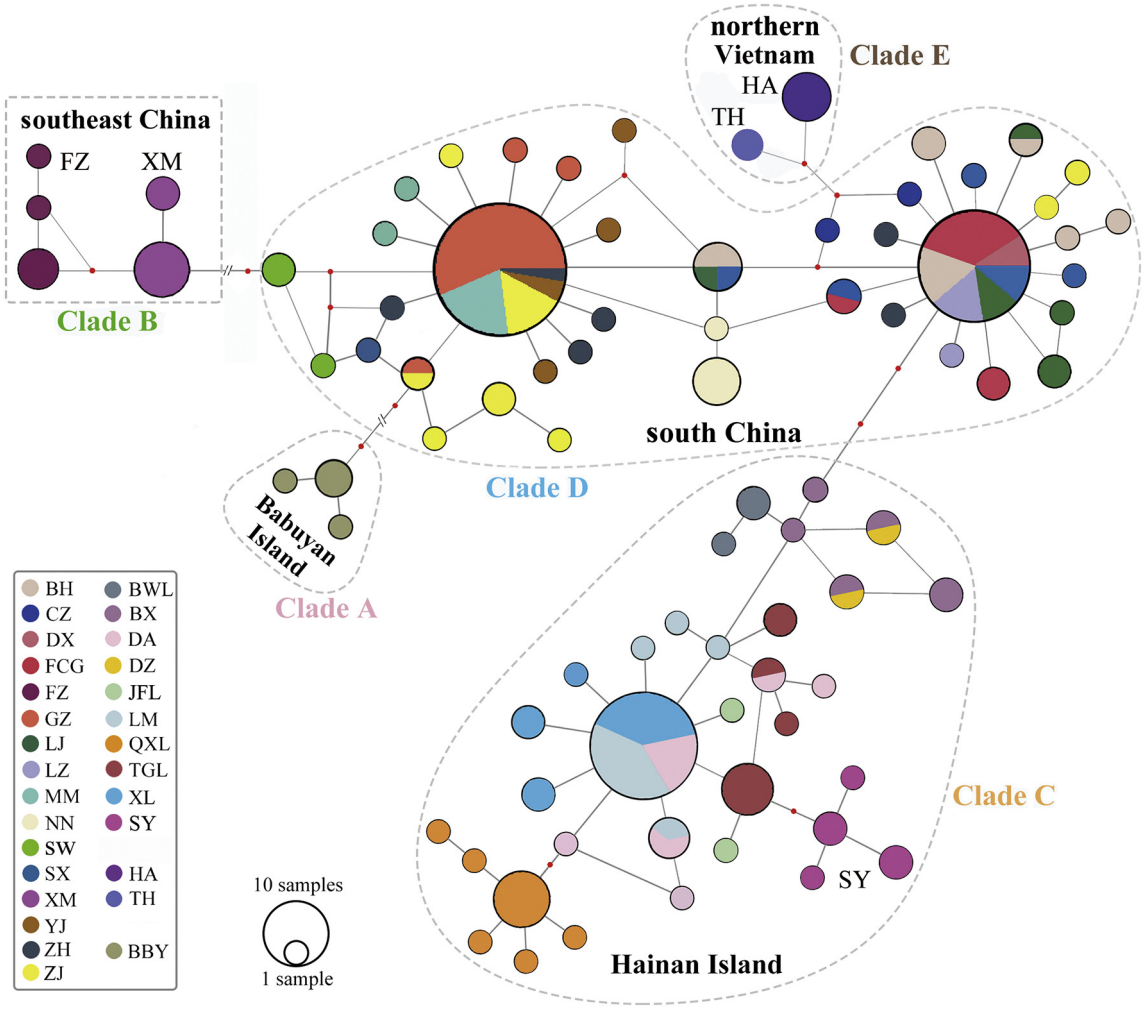

Fig. 3. Network profile. Network profile based on *COI* gene of 28 populations. Each haplotype is represented by a circle. The size of the circle is proportional to that haplotype's frequency. Colours denote lineage membership and are the same as in Fig. 1. (For interpretation of the references to colour in this figure legend, the reader is referred to the online version of this chapter.)

3.1. Associations between genetic diversification and phylogeographical structure in continental area

Geographical isolation (due to distance, water and mountains) separates populations, impedes gene flow, and generates genetic differentiation, which has been leading to the evolution of new species (viz, allopatric speciation) in almost all animal groups (e.g., mammals, birds, frogs and cicadas) [34,36,37]. Rivers have acted as substantial barriers to gene flow within numerous species of insects distributed in East Asia [34]. Our present study based on combined maternally inherited mitochondrial DNA and bi-parentally inherited nuclear genes provides a comprehensive framework to analyse the phylogeography and demographic history of *P. hilpa*. The population structure of *P. hilpa* comprises five large units with high genetic diversity and obvious hierarchy (Figs. 2, 3). Both phylogenetic and phylogeographical analyses indicate significant genetic/geographical isolation among these divergent lineages (Figs. 2, S2, S3). This implies that geological events, coupled with past climatic oscillations (see below), play an important role in driving genetic patterns and differentiation of this cicada species.

The species *P. hilpa* is primarily distributed in coastal areas of southern China and northern Vietnam, and also occurs in adjacent islands such as Hainan Island and Babuyan Island (Clades A–E) (Fig. 1a). The BBM analysis in our study identified "south China" as the ancestral species range with high probability, and suggested two independent, contemporaneous colonizations from there to southeast China and northern Vietnam (Fig. 7). The species extends northeastward to

Table 2
Analysis of molecular variance (AMOVA) for mtDNA data among the five groups ($K = 5$) and four groups ($K = 4$) in *P. hilpa* defined by SAMOVA.

Gene(s)	Source of variation	d.f.	Sum of squares	Variance components	Percentage of variation	Fixation indices
COI	Among groups	4	599.822	8.35487Va	71.43	Φ_{CT}:0.79325
	Among populations within groups	10	41.358	0.70154Vb	19.35	Φ_{SC}:0.49687
	Within populations	123	59.412	0.43314Vc	9.22	Φ_{ST}:0.88547
COI + COII + Cytb	Among groups	3	646.521	16.25483Va	82.13	Φ_{CT}:0.76241
	Among populations within groups	9	192.324	2.15264Vb	15.11	Φ_{SC}:0.85648
	Within populations	93	129.35	0.89654Vc	2.76	Φ_{ST}:0.59341

Significance test: 1000 permutations; d.f.: degrees of freedom; Va, Vb and Vc indicate the difference level; All values were significant at $p < .01$.

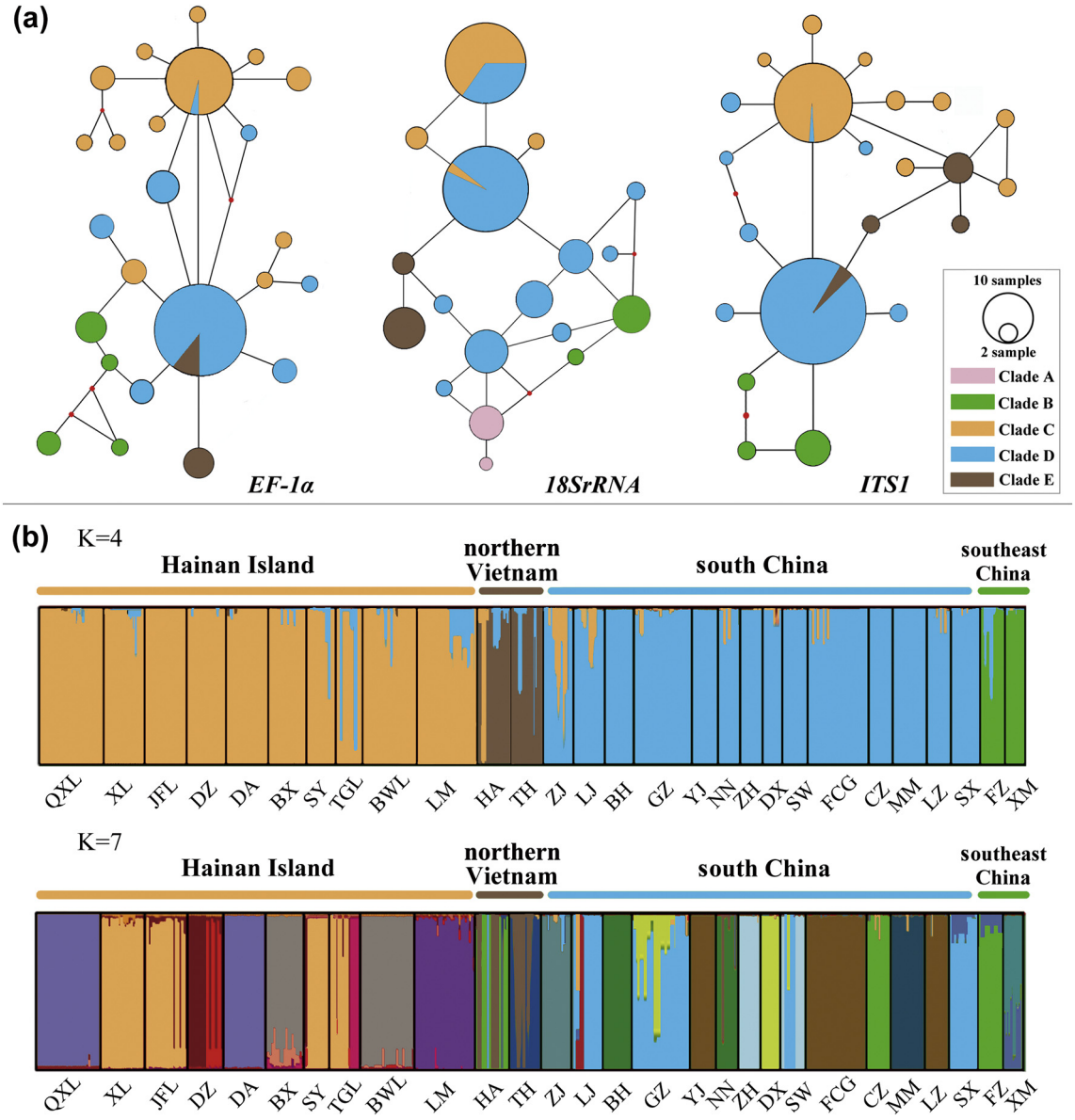

Fig. 4. Population structure of *P. hilpa*. (a) Network profile based on nuclear genes (*EF-1α*, *18S* and *ITS1* gene, respectively). Each haplotype is represented by a circle. The size of the circle is proportional to that haplotype's frequency. Colours denote lineage membership and are the same as in Figs. 1a, 2. (b) Results of genetic assignments based on variations at six microsatellite loci obtained using the Bayesian methods implemented in the program STRUCTURE. Individual specimens from the 28 populations were grouped into four main clusters (K = 4); histogram of the STRUCTURE analysis for the model with K = 7. See Table 1 for the explanation of the population codes. (For interpretation of the references to colour in this figure legend, the reader is referred to the online version of this chapter.)

southeast China (Fujian Province), where the populations (e.g., XM and FZ populations) form an ecologically and phylogenetically distinct group (Clade B) and are separated from other lineages by the Wuyi Mountains and Peale River (Fig. 1). The Wuyi Mountain ranges, one of the oldest ranges in the coastal regions of southeast China, are continuously distributed in a southwest-to-northeast orientation [38,39]. The Wuyi Mountains not only represent a major dispersal and climatic barrier for organisms [39,40], but also have historically provided refugia for plants and animals, as the Quaternary glaciation has not occurred there [41,42]. Our results suggest that the Wuyi Mountains and the Peale River appear to have promoted the divergence of the southeast China lineage of *P. hilpa* from other lineages.

We obtained similar results when estimating the divergence time of *P. hilpa* by using BEAST* (concatenated mtDNA genes) and BEAST (combined *COI* and *18SrRNA* genes, calibration value 1.55 ± 0.15 Ma) (Fig. 5). Therefore, we mainly focus on the chronogram of *P. hilpa* based on BEAST to analyse the divergence time of related lineages of *P. hilpa*. During the mid-Pleistocene (~0.88 Ma), the Vietnamese lineage (Clade E) was split from the south China lineage (Clades D1–D4), and formed an ecologically and phylogenetically distinct group (Figs. 1a, 5). A well-known geological process occurred in Asia during the predicted period and geographical area, the south-eastern lateral extrusion of the continental landmass under the pressure of the colliding Asian and Indian plates, is thought to be linked with these cladogenic events [43–45]. These tectonic movements occurred during the Oligocene and early Miocene starting at approximately 34–30 Ma and, then, lateral extrusion and shearing between 26 and 17 Ma provoked extensive faulting and folding of the upper crust in southern China and northwestern Vietnam [44,46,47]. This event eventually generated the Song Chay detachment faults and Ailao Shan–Red River shear zone [43,48,49], and the local biota has been influenced by this major discontinuity [50].

Our results, which were inferred using a comprehensive range of populations of *P. hilpa*, support the key role the geological event played in

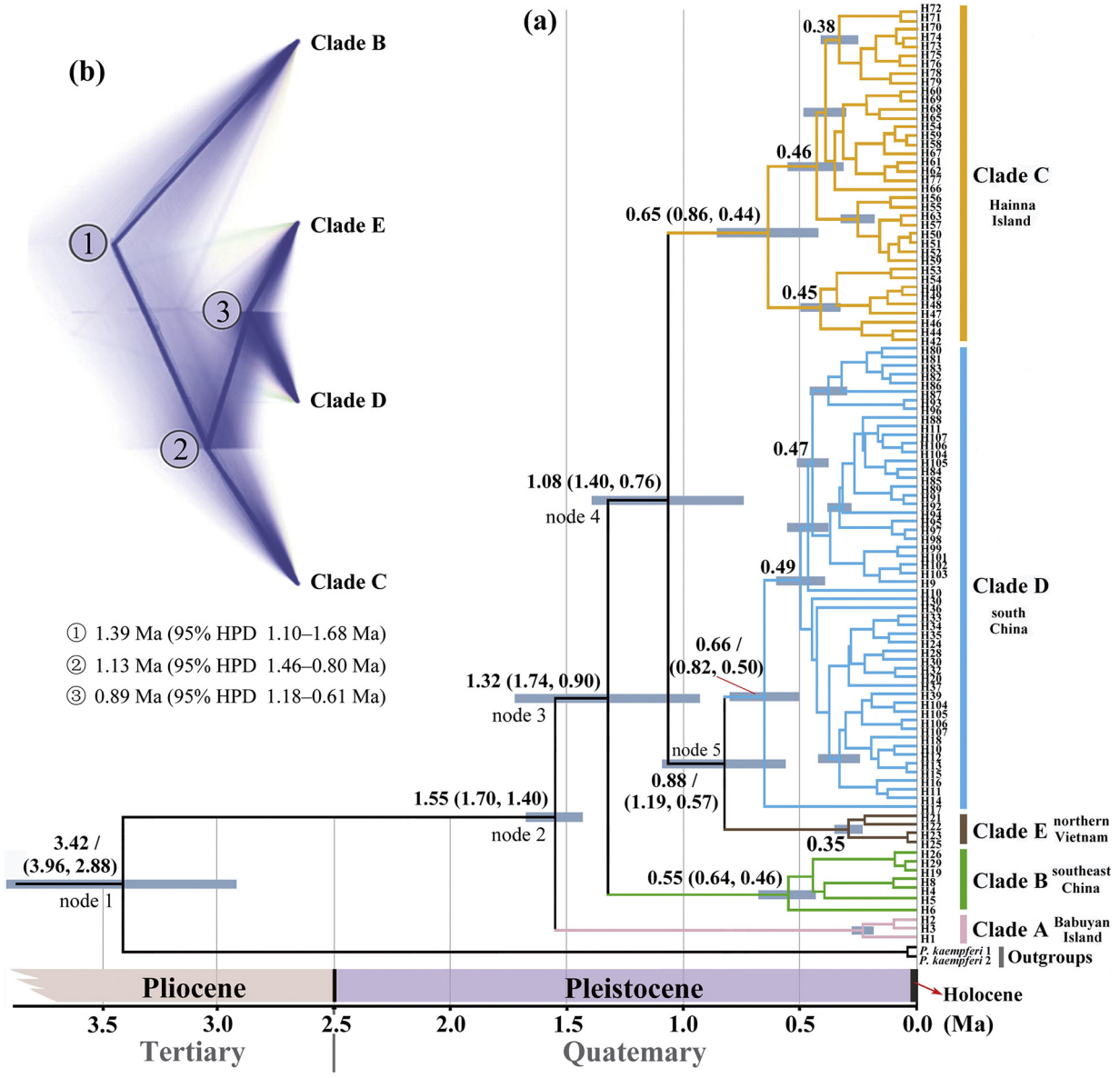

Fig. 5. BEAST-derived chronograms. (a) The divergence time of *P. hilpa* and outgroup taxa based *COI* and *18SrRNA* gene sequences, constructed using BEAST and drawn by FigTree. Blue bars indicate the 95% highest posterior density (HPD) credibility intervals for node ages (in Myr ago, Ma). (b) Species tree analysis implemented in *BEAST based on concatenated (*COI* + *COII* + *Cytb*) genes, estimated by *BEAST. Darker branches represent a greater proportion of corresponding trees. Consensus trees are presented by solid lines.

shaping the early phylogeny of this cicada species. Regarding the region of northeast Vietnam where it is contiguous to southern China, previous studies on some invertebrate species suggest that the fauna there is more similar to that of south China instead of northern Vietnam [6]. Therefore, the distributions of *P. hilpa* in northeast Vietnam and south China are put together into the same distribution range in our BBM analysis of ancestral distribution areas (B in Fig. 7a). We infer that the mountains (e.g., Shiwanda Mountains) located in the border area between China and Vietnam, together with the Song Chay detachment faults and Red River delta (Fig. 1), have been serving as effective geographical barriers to the dispersal and gene flow of *P. hilpa*. Given that *P. hilpa* is mainly distributed in the coastal areas of southern China, northern Vietnam and adjacent islands but does not occur in other areas of the Indo-China Peninsula [41,43,51,52], we further infer that the geographical barriers between northern Vietnam and other remaining areas of the Indo-China Peninsula (e.g., Fansipan and Phu Luong Mountains) have not only split the ancestral distribution of *P. hilpa* there, but also have played an important role in impeding the further southward spread of this species.

3.2. Impact of past climate change on genetic divergence and phylogeography of populations of Hainan Island and the adjacent mainland

Past climatic oscillations coupled with geological events have played important roles in forming the contemporary genetic diversity and population structure of animals across the globe [2,10], but most subtropical and tropical regions were not glaciated during the Pleistocene [53]. *Platypleura hilpa* represents a typical insect species in subtropical and tropical Asia, but how this species responded to past environmental change remained unknown. Our analysis of population structure of *P. hilpa* based on the single *COI* gene and also combined mtDNA revealed significant differentiation for populations that occurred in Hainan Island and the adjacent mainland (Figs. 2, 3, S2). Our results based on nuDNA and SSR data indicate an intraspecific gene flow among related populations of *P. hilpa*. Obviously, the Qiongzhou Strait forms a natural barrier to the gene flow (Figs. 1a, 4). BEAST analyses (Fig. 5) indicate that the Hainan populations split from the mainland populations at an estimated time of ~1.08 Ma (95% HPD: 0.76–1.40). This is coincident with the

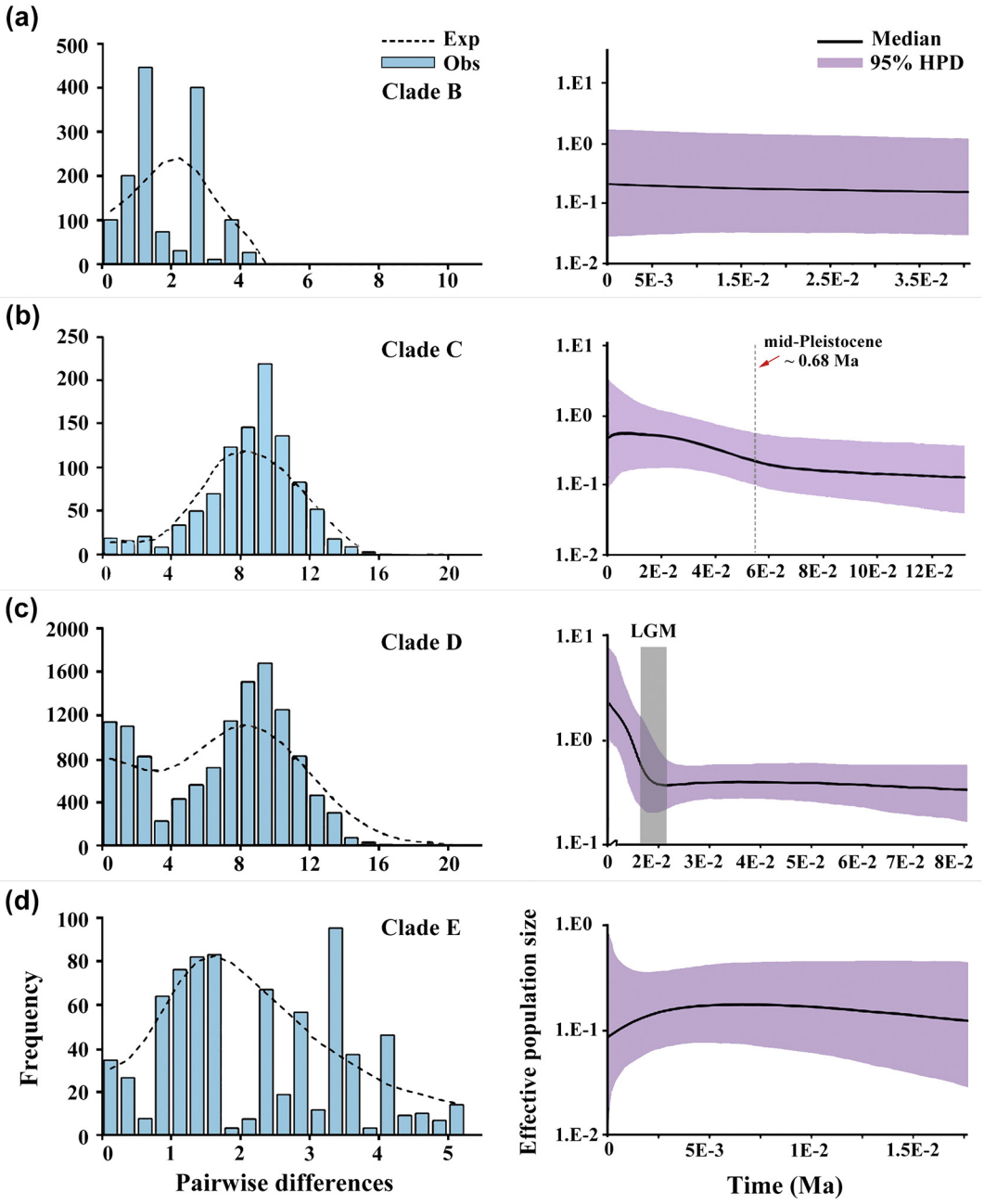

Fig. 6. Mismatch distributions (left) and Bayesian skyline plots (right) of four clades (Clades B–E) of *P. hilpa*. The x axis is in units of millions of years ago. The y axis is equal to the effective population size. Estimates of means are joined by a solid line, whereas the upper and lower lines delineate the 95% HPD limits. E means a natural constant and is approximately equal to 2.718. LGM, Last Glacial Maximum.

early-to-mid-Pleistocene, during which glacial cycles led to sea-level fluctuation [2,20]. One of the most important factors for interpreting this population structure could be the role of the Qiongzhou land-bridge (i.e., the exposure or submergence of the South China Sea Shelf) [45,54]. The Qiongzhou land-bridge repeatedly amalgamated Hainan Island with the adjacent mainland during glacial periods when sea levels were lower [45,46,55]. It is plausible that *P. hilpa* had reached the island via dispersal and, with geographic isolation fostering speciation, ancestral populations there could have evolved into ecologically and phylogenetically independent groups. Genetic admixture between mainland and island populations could have occurred possibly up to the last glacial period with the most recent land-bridge. This admixture scenario is corroborated by the Ecological Niche Modeling (ENM), which reveals a band of suitable LGM habitat extending from south China across the Qiongzhou land-bridge to Hainan during the LGM (Fig. 8b). Correspondingly, continental nuDNA haplotypes are found in *P. hilpa* populations occurring on Hainan Island, which reflect strongly asymmetrical nuclear introgression from mainland populations into island populations, with selection against immigrant nuDNA. In addition, our results show that the populations of Hainan are most closely related to those from south China, but are distantly related to populations of northern Vietnam (Figs. 2–4). This suggests that the Beibu Gulf (previous Gulf of Tonkin, shown in Fig. 1) represents a more important geographic barrier than the Qiongzhou Strait to gene flow among *P. hilpa* populations.

Island-mainland distributions have often been considered a model for the study of isolation and genetic divergence [56]. Compared to their mainland counterparts, island populations are generally characterized as having lower genetic variation, less among-population differentiation, more significant inbreeding, and a much higher risk of

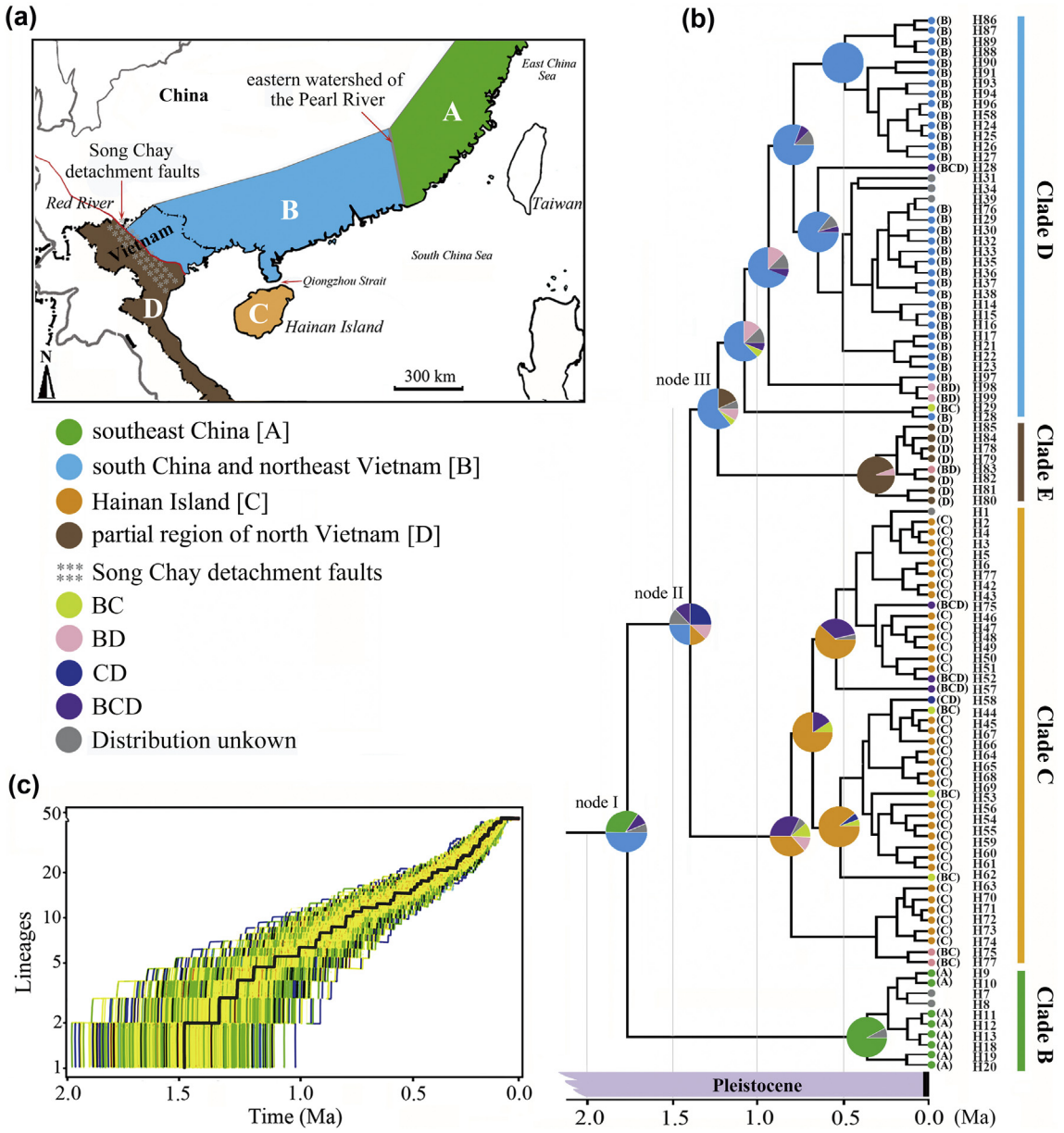

Fig. 7. Biogeographical ancestral optimization performed with statistical dispersal-vicariance analysis (S-DIVA) and Bayesian binary MCMC (BBM). (a) Distribution map of the four delimited areas (A–D) used herein. (b) Combined results of the ancestral area reconstructions: coloured pie charts at the nodes indicate the probability of ancestral areas inferred using a parsimony-based statistical dispersal–vicariance method (S–DIVA). (c) Lineages-through-time (LTT) plot with 95% confidence interval of *P. hilpa*. Biogeographical regions: A, southeast China; B, south China and northeast Vietnam; C, the Hainan Island; D, partial region of north Vietnam. (For interpretation of the references to colour in this figure legend, the reader is referred to the online version of this chapter.)

extinction [57,58]. The general effects of episodes of warming and cooling during the Pleistocene on genetic diversity and structure of tropical and subtropical species remain largely unclear, especially for endemic taxa of islands. Hainan Island, known as a biodiversity hotspot in East Asia [28], is located in the transitional zone between tropical and subtropical regions in the South China Sea. Its fauna has always received increased attention because of the special geographical location and the diversified ecological environments [59,60]. The topography of Hainan Island is diverse, with Wuzhi and Yinggeling Mountains approaching elevations of 1800 m, rising steeply from the central and southern regions and giving way to a broad plain in the north (Fig. 1b). Our molecular analyses revealed that the population structure of the Hainan lineage of *P. hilpa* comprises four subclades with high genetic diversity and obvious hierarchy (Clades C1–C4) (Figs. 1b, 2a, 3). High genetic differentiation is observed among SY, QXL and remaining populations of Hainan Island (Fig. 1b), suggesting that the Wuzhi and Yinggeling Mountain ranges have been important barriers limiting gene exchange among populations on different sides of the mountain series. As mentioned above, continental nuDNA haplotypes are found in *P. hilpa* populations of Hainan Island, but no continental mtDNA haplotypes are found from the island populations. This reflects how high levels of genetic drift and extinction occurred in the island populations, and/or that strongly asymmetrical nuclear introgression from mainland populations into island populations occurred with selection against immigrant mtDNA [61].

3.3. Long-distance dispersal of cicadas across the ocean

Platypleura hilpa is patchily distributed in the coastal areas of southern China, northern Vietnam and many islands adjacent to the mainland (e.g., Hainan, Mazu, Jinmen and Penghu Islands, shown in Fig. 1), but does not occur in Taiwan Island [41,51,52]. Recently, Osozawa et al.

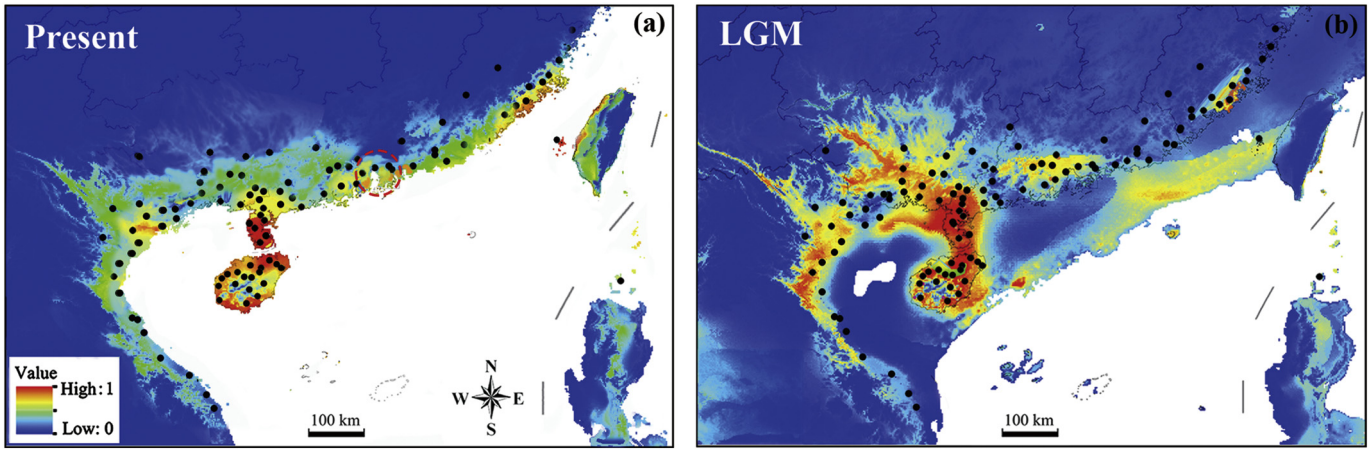

Fig. 8. Potential distributions as probability of occurrence for *P. hilpa* in subtropical China mainland, Hainan Island and northern Vietnam. (a) The suitable areas for *P. hilpa* during the under present conditions (1950–2000). (b) At the Last Glacial Maximum (LGM). Ecological niche models were established with present bioclimatic variables on the basis of extant occurrence points (black dots) of the species using MAXENT.

[35] discovered *P. hilpa* from Babuyan (BBY) Island and the Luzon Volcanic Arc of the Philippines, where the majority of islands are younger and have origins in the Quaternary (~1.55 Myr) [62]. There is an active backarc basin of the Okinawa trough in front the East China Sea, which started spreading at ~1.55 Ma, leading the forearc area including the Ryukyu Islands to be subsided [62]. The continental shelf was reflected by eustatic sea-level change after ~20.5 Ma when the South China Sea (back arc basin) ceased sea floor spreading [45]. In addition, there was no mountain building process and sea floor spreading during this period [45]. Given that the Babuyan Island has never been geographically connected to Taiwan and the adjacent mainland due to the absence of a land-bridge there [63], and that cicadas do not have the ability for long-distance dispersal across the ocean [31], a question which is raised is: how did *P. hilpa* disperse long-distance across the ocean from the mainland and/or adjacent islands to Babuyan Island? Although our analyses did not include the *P. hilpa* population from Penghu Islands, we proffer that there is a close affinity between this population and the populations occurring in Xiamen (XM) Island due to their very close geographical affinity (~140 km). However, our molecular phylogenetic analyses revealed that the Babuyan population is more closely related to populations from South China (e.g., ZJ population of Guangdong Province) rather than to the XM population. Phylogenetic trees based on combined (*COI* + *18S*) genes (Fig. 2b) and *COI* gene haplotype network (Fig. 3) both imply possible historical dispersal events for *P. hilpa* from south China to Babuyan Island, as the haplotype from the latter occupies "tip" (derived) positions relative to the ancestral haplotype from the former (south China). Divergence time analysis (Fig. 5a) suggests that the BBY clade might have been separated from a common ancestor in the Pleistocene (~1.55 Ma) when Taiwan and Penghu Islands were linked to the mainland due to the fall in sea-level [62]. But then again, as the Babuyan Island and Luzon Islands has never been geographically combined to Taiwan and the adjacent mainland due to the absence of any land-bridge there [63], we infer that the distribution of *P. hilpa* on the Babuyan Island might have been caused by long-distance dispersal through rafting. This pattern of long-distance dispersal across oceanic barriers is a rare event, but strong storms and ocean currents can drive these stochastic processes [64]. Rafting of terrestrial organisms to remote oceanic islands has been reported from a range of floating substrates and across all major oceans of the world [65]. For example, previous studies have indicated that cross-oceanic dispersal of a few flightless weevils could have resulted from oceanic currents [63]. Our field investigations reconfirmed that *P. hilpa* females oviposit in the dead twigs of its host-plant *Ficus microcarpa* Linn. F. [66]. This plant is a common monoecious tree, widely distributed in the fig center area of Asia-Australasia [67]. It is possible that *P. hilpa* might have colonized the Babuyan Island belt after its eggs harbored in the twigs of host-plants had been rafted on floating substrates from the mainland (most possibly south China).

Regarding the distribution of *P. hilpa* only on the Penghu Islands but not on the neighboring Taiwan Island, one explanation could be that *P. hilpa* has dispersed to Taiwan but went extinct. This scenario is supported by the ENM, which reveals a band of suitable LGM habitat extending from south China across the South China Sea Shelf to the Penghu Islands as well as the west coastal area of Taiwan (Fig. 8b). An alternative explanation could be that this species never spread southeastward to Taiwan Island.

3.4. Historical demography

The glacial cycles of the Quaternary resulting in climatic oscillation and sea-level fluctuation had a significant influence on the evolutionary history and contemporary distribution patterns of current species in Vietnam and China, even if this area was not completely covered by ice sheets [53,68]. Results of our study indicate that the Hainan Island lineage of *P. hilpa* (Clade C) shows a "star-like" pattern characteristic of population expansion, which is confirmed by our Bayesian skyline results (Table S3; Figs. 3, S2c). As this expansion signal is dated to the mid-Pleistocene (0.68 Ma, 95% CI: 0.39–0.97) (Fig. 6b), it clearly indicates that this species might have benefited from a host-plant expansion as a result of the warmer and more humid climates promoted by a stronger Asian summer monsoon during the early Pleistocene in Hainan Island and adjacent areas [59,66]. In addition, the glaciation periods, as well as the accompanying lowering and rising of sea levels during the Pleistocene, are known to have greatly affected land mass configurations and plant and animal distributions in Southeast Asia [69]. The populations of *P. hilpa* from south China show genetic imprints of a demographic expansion as inferred by a negative Tajima's *D* test and Fu's *Fs* test, which is supported by the mismatch distribution analysis and Rogers test of sudden population expansion [70] (Table S3; Fig. 6c). This expansion time is estimated to be LGM (Fig. 6c). Maxent models indicate (Fig. 8b) that this intensification of the subtropical monsoon climate would have increased levels of precipitation in south China due to the formation of land-bridges across the South China Sea [71]. Consequently, the suitable habitats of *P. hilpa* as well as its host plants might have expanded southward along with the South China Sea Shelf, resulting in a rapid population expansion of *P. hilpa* during the LGM (Fig. 8b).

The rise of the Tibet–Qinghai Plateau is believed to have had a profound impact on organisms on the Tibetan Plateau itself and neighboring areas including Guangxi Province, Guangdong Province and

Hainan Island [72,73]. The distribution pattern of *P. hilpa* in the mainland of Southeast Asia indicates that the Yunnan-Guizhou Plateau, Nanling Mountains and Wuyi Mountains are obstacles to the dispersal of this species northward, which might be closely related to the post-glacial development of flora of Southeast Asia [39,40]. Given that this cicada species is patchily distributed in the coastal areas, we infer that historical climate changes together with climate-related sea-level changes mainly shaped the current distribution pattern and genetic divergence of *P. hilpa*, as sea level fluctuations could have led to local extinctions of some populations or caused populations to be isolated depending on the size of a land mass and its connectivity to other land masses. Subsequent dispersal and accumulation of genetic differences of *P. hilpa* over time are possible evolutionary mechanisms that account for the genetic divergence we observed.

3.5. Potential impacts of climate and environment change based on ENM evidence

Past climate change at larger scales has influenced dispersal and range shifts in many taxa [74]. During the past three million years global climate has fluctuated greatly, resulting in the recent major ice age and substantial changes in the distributions of many living organisms in temperate and tropical zones [2,5]. Such changes include fragmentation of previously contiguous habitats of populations in animals, which might have resulted in both genetic and behavioral divergence. Climate is often thought to be the predominant range-determining mechanism at large spatial scales [75]. In particular, habitat loss affects the spatial pattern of residual habitat and induces microclimatic changes and habitat fragmentation [76]. Habitat fragmentation is a major threat to the survival of natural populations and to the functioning of ecosystems, which consequently leads to species endangerment, extinction, and biodiversity loss [77,78]. The single-refugium hypothesis generally is based on a star-like haplotype network in the whole population and would present decreasing trends on genetic diversity from one single refugium to the newly colonized routes and/or fringe areas [79]. However, this pattern was not found for *P. hilpa*.

Our present study suggests that *P. hilpa* is likely derived from multiple glacial refugia rather than a single refugium, as several lines of evidence support the scenario of multiple glacial refugia at least in Hainan Island and southern China. In detail, not only the mtDNA data but also the nuDNA data in our study revealed two major distinct haplotype groups (Figs. 3, 4, S2); and especially based on the mtDNA data, the two lineages (Clade C and Clade D) independently possessed high genetic diversity (Table S3). As mentioned above, the divergence of these two lineages dated back to the early Pleistocene, which is much earlier than the LGM, implying that they had occupied independent glacial refugia where stable suitable environments could have been maintained through history [80]. In particular, our ENM of present and paleo periods (LGM) indicates that stable suitable habitats through time for *P. hilpa* existed in both Hainan Island and southern China (Fig. 8). The ancestral area distribution of *P. hilpa* indicates that the most recent common ancestor of the populations in these areas were relatively old (Fig. 7b). It is therefore plausible to postulate that these regions had been occupied as the refugia for different lineages of *P. hilpa*.

Regarding the host plants, *P. hilpa* is specialized to live on *Ficus microcarpa* Linn. F., a common evergreen and native species in subtropical China [81] and also a main tree species in the tropical forest [67]. Although Chen [82] recorded that *P. hilpa* was observed perching on *Casuarina equisetifolia* Forst in the windbreak forest of Penhu Island, the author did not note whether this plant is the host plant for this cicada species or not. The population divergence, vicariance and evolutionary history and, in particular, the current distribution of *P. hilpa* should be definitely closely related with the historical and current distribution of its host plant *F. microcarpa*. We propose that Pleistocene sea-level fluctuations had profound effects on lineage diversification and the regional genetic structure of this cicada species. The demographic history of this species was influenced by habitat requirements and changes in climate during the last glacial maximum, which might have also affected the distribution of the host-plant *F. microcarpa*. Our study highlights the importance of physical barriers, such as mountains, rivers and straits, in shaping the present-day distribution of a species at lower latitudes, and provides insights into revealing potential impact of geological events on insects in subtropical and tropical coastal areas of southern China and the northern Indo-China Peninsula. The outcome of our analyses will contribute to a better understanding of the pressures climatic change imposes on insects occurring in these areas, particularly those with a long, subterranean pre-adult stage and low dispersal ability in the adult stage..

4. Materials and methods

DNA extraction, amplification, sequencing in combination with microsatellite genotyping methods, ecological niche modeling (ENM) and key environmental variables are described in supplemental materials.

4.1. Specimen collection

In total, 361 individuals of *P. hilpa* were sampled from 28 localities from coastal areas of southeast China (SEC), south China (SC), northern Vietnam (NV) and Hainan Island (HN) (Fig. 1) (Table 1). Consecutive samples at a location were collected a minimum of 100 m apart, or in different fields, to minimize the chance of sampling *P. hilpa* from the same colony. After capture, two legs of each individual were immediately removed, placed in 95% ethanol and later transferred to a − 80 °C freezer. Two congeneric species, *Platypleura kaempferi* (Fabricius) and *P. assamensis* Atkinson, were chosen as outgroup taxa for phylogenetic analyses. All specimens used for molecular identification and phylogenetic analysis are listed in Table 1.

Sequenced voucher specimens, except for those of the Babuyan Island (BBY) population, were deposited in the Entomological Museum of Northwest A&F University (NWAFU), Yangling, China.

4.2. Phylogenetic analyses

The most suitable partitioning strategies and evolutionary models for each partition were estimated using the program PARTITIONFINDER v1.1.1 [83] by giving the program different potential groups of 1st, 2nd, and 3rd codon positions of protein-coding genes. The Bayesian Information Criterion (BIC) was used to compare alternative partitioning schemes and sequence models. Maximum likelihood (ML) analysis was executed with the program raxmlGUI v1.3, a graphical front-end for RAxML [84]. All ML analyses with the "thorough" bootstrap setting were run ten times starting from random seeds under the GTR + I + G model. This was repeated until the likelihood score and parameter estimates no longer changed. Trees were initially estimated under maximum parsimony by stepwise random addition with tree bisection-reconnection (TBR) branch swapping on ten replicates, keeping the best tree only. Bootstraps [85] were conducted for the ML analyses using the final parameter settings for 100 pseudo replicates, saving the best tree from ten search replicates per bootstrap replicate. The bootstrap support value (BS) was evaluated by analysis with 1000 replicates. Concatenated mitochondrial and nuclear genes (*COI* + *COII* + *Cytb* + *EF-1α* + *18S* + *ITS1* and *COI* + *COII* + *Cytb*) to gain further insight into the population genetic structure of *P. hilpa* occurring in China and Vietnam. Individual loci (*COI* and *18S*) genes were analysed independently to reconstruct phylogenetic trees of all populations before combining them.

BI analysis was conducted using MRBAYES v3.1.2 [86]. The Markov chain Monte Carlo (MCMC) algorithm was run for 2000,000 generations, with four incrementally heated chains. The analysis involved starting from a random tree and sampling every 100 generations. The

average standard deviation of the split frequency among runs was lower than 0.01, indicating that the sampling of the posterior distribution was adequate. The average standard deviation of split frequencies and the Potential Scale Reduction Factor (PSRF) were used for examining convergence. The stationarity was determined with the program TRACER v1.5 [87] by plotting the log-likelihood values versus generation number. After the first 25% of the yielded trees were discarded as burn-in, a 50% majority-rule consensus tree with the posterior probability values was constructed by summarising the remaining trees.

4.3. Genetic diversity and population structure analyses

The haplotypes were defined using DNASP v5.0 [88] based on the mitochondrial genes and nuclear genes. Genetic diversity was estimated using DNASP v5.0 by computing haplotype diversity (h) and nucleotide diversity (π). To further investigate the relationships among unique haplotypes, unrooted networks were constructed using two methods: the neighbor-net algorithm with SPLITSTREE v4.6 [89], and a median-joining method constructed with default settings in NETWORK v5.0 [90]. The data of the combined mitochondrial genes and three nuclear genes were concatenated respectively for analysis of the China and Vietnam populations, as well as *COI* gene for all populations. In order to test genetic barriers and to define groups of populations, SAMOVA 2.0 was used to analyse spatial molecular variance, without prior structure parameters [91]. The proportion of total genetic variance (F_{CT}) was maximised by the spatial analysis of molecular variance (SAMOVA) because it was different between population groups to predefine number of groups (K). SAMOVA was run with K from 2 to 9 on the basis of simulated annealing steps. In order to estimate genetic variation level among and within groups, AMOVA [92] was carried on in SAMOVA. The significance of variance components was detected with permutations. A three-level hierarchical analysis of molecular variance (AMOVA) was performed with genetic variation and fixation indices Fst values implemented in ARLEQUIN v3.5 [93] by computing conventional F-statistics from haplotypes with 1000 permutations. Multiple methods were performed to understand the population genetic structure of *P. hilpa*. First, pairwise Fst was examined using ARLEQUIN v3.5 between each pair of the sampled populations; then, Mantel tests of the genetic distance [Fst/(1-Fst)] vs the geographical distance (ln km) based on mitochondrial genes calculated with the software ZT v1.1 [94] were conducted to estimate the level of isolation by distance.

The individual-based genetic structure of the SSR loci was also evaluated. The number of *P. hilpa* populations was determined using a Bayesian genotypic clustering method in STRUCTURE v2.3.3 [95]. Mean values were calculated from 10 simulations for each model (k ¼ 2–7) assuming admixture and correlated allele frequencies between populations with a 500,000 replications burn-in period and 500,000 Markov Chain Monte Carlo replicates. As suggested by Hubisz et al. [96], sampling locality was set as a priority to magnify potential signals of population structuring. The criteria identifying the most likely number of clusters followed Pritchard et al. [97] and Evanno et al. [98]; the evaluation conducted in the website of STRUCTURE HARVESTER [99]. CLUMPP v1.1.2 [100] was carried out to merge the results from replications of each K, and bar plotting results were created with DISTRUCT v1.1 [101].

4.4. Divergence time estimation

The divergence times for the haplotype lineages based on combined *COI* and *18SrRNA* genes were estimated using the software BEAST v1.8.2 [102]. As presented in Osazawa et al. [62], the Ryukyu Islands were isolated from China at 1.55 Ma which were not gradually separated, but synchronously subsided (but not completely submerged). After carefully consideration, the differentiation between each of the most recent common ancestor (MRCA) of the endemic *P. hilpa* of the Babuyan Island population and the remaining lineages, began at 1.55 ± 0.15 Ma based on the geological evidence for island separation, was used, i.e., a date of 1.55 ± 0.15 Ma was input into BEAUti for the time to MRCA for *P. hilpa*. Running BEAST was done by incorporating each xml input file made by BEAUti. TRACER v1.5 [87] was used to verify the posterior distribution and the effective sample sizes (ESSs) from the MCMC output. TREEANNOTATOR v1.10 was used to find a maximum credibility tree with the annotation of mean node ages and the 95% highest posterior density (HPD) intervals [103]. We assessed whether a ESS > 200 was achieved for all parameters after the analyses. The tree with divergence time estimates was displayed using FIGTREE v1.4.3 [104]. The same settings for three independent runs were used in order to ensure the consistency of the results.

Because an uncalibrated molecular clock analysis can offer a way to estimate approximate divergence times, although it is not ideal, when no calibration information (e.g., fossil data) are available [32,34,105], we also used *BEAST to estimate divergence time based on all of the concatenated mitochondrial sequences to further test the lineage divergence time revealed in the mitochondrial haplotypes [106]. The proposed conventional mutation rates for insect mitochondrial *COI* gene 2.3% per million years (i.e., 0.0115 substitutions/site per lineage) was used [107]. The set of parameters was the same as that used with the mitochondrial haplotypes.

4.5. Demographic history analysis

Demographic history was analysed for all the groups identified via the package DNAsp. We calculated Tajima's D (D) and Fu's Fs statistic, and ran 10,000 coalescent simulations for each statistic to create 95% confidence intervals to investigate the historical population demographics and test whether the sequences conformed to the expectations of neutrality. Pairwise mismatch distribution analyses were performed to find evidence of past demographic expansions using DNASP v5.0. Historical demographic trends were investigated through a mismatch distribution analysis using ARLEQUIN v3.5 to detect expansion through the linear fitting of observed and simulated curves with the significance of two parameters (SSD and Hrag). The population history was also investigated by estimating the changes in the effective population size over time using a Bayesian skyline plot [108] implemented in the software BEAST v1.8.2. This approach incorporates uncertainty in the genealogy using MCMC integration under a coalescent model. The piecewise-linear skyline model was selected for the Bayesian skyline coalescent tree priors. Chains were run for 200 million generations with a sampling every 20,000 generations. The convergence and output of BEAST were checked and analysed using TRACER v1.6.

4.6. Ancestral area reconstructions and diversification rate through time

Bayesian binary MCMC (BBM) analysis and statistical dispersal-vicariance analysis (S-DIVA) implemented in RASP v3.0 [109] were conducted using trees retained from the intraspecific BEAST analysis to reconstruct the geographical diversification of *P. hilpa*. In order to prevent biasing inferences towards wide or unlikely distributions, the outgroup was pruned for ancestral state reconstructions. According to the distribution range of the four phylogroups, the distribution range of *P. hilpa* was divided into four main areas (A, southeast China; B, south China and northeast Vietnam; C, Hainan Island; D, partial region of north Vietnam; the eastern watershed of Pearl River is the boundary of A and B, and the Song Chay detachment faults separate B and D) (Fig. 7a). The DIVA method was used in a statistical context by these two analyses to calculate the probability of ancestral areas over a Bayesian posterior distribution of tree topologies. Given phylogenetic uncertainty, the estimation of ancestral area marginal probabilities has been suggested to decrease uncertainty in the biogeographical reconstruction [110]. The number of maximum areas at each node was set to six. To account for phylogenetic uncertainty, 5000 out of 20,000 post-burn-in trees from BEAST were randomly chosen for BBM analyses

[111]. The root distribution was set to null, 10 MCMC chains was applied with the F81 + Γ model running for 10^6 generations, and sampled the posterior distribution every 100 generations; the first 25% sampled were discarded as burn-in.

To account for phylogenetic uncertainty, 1000 randomly selected trees we used from the postburn-in BEAST trees. Parsimony reconstruction was conducted in MESQUITE 3.04 [112] by using the 'trace character over trees' option and unordered character state transformations. A multiple lineage-through-time plot (LTT) was used to display the overall pattern of diversification in *P. hilpa* graphically. Each plot was implemented with the R package APE [113] using a 1000 random tree-set derived from the BEAST output and the consensus chronogram arranged for the ancestral state reconstruction, removing time by time the outgroup samples and unnecessary species of *P. hilpa*.

CRediT authorship contribution statement

Yunxiang Liu: Methodology, Software, Data curation, Writing-original draft, Visualization, Investigation. **Hong Thai Pham:**Visualization, Investigation. **Zhiqiang He:** Visualization, Investigation. **Cong Wei:** Conceptualization, Supervision, Writing-review & editing.

Declaration of competing interest

The authors have no conflicting interests.

Acknowledgements

The authors would like to give thanks to Dr. Soichi Osozawa (Tohoku University, Japan) and Dr. Myron Zallucki (University of Queensland, Australia) for providing valuable comments on a previous version of this manuscript, and to Dr. Masami Hayashi (Tokyo University of Agriculture, Japan) for providing information on the host-plant of the cicada *Platypleura hilpa*. This work was supported by the National Natural Science Foundation of China (Grant No. 31772505).

Appendix A. Supplementary data

Supplementary data to this article can be found online at https://doi.org/10.1016/j.ijbiomac.2020.02.183.

References

[1] G.S. Doorn, P. Edelaar, F.J. Weissing, On the origin of species by natural and sexual selection, Science 326 (2009) 1704–1707.
[2] G.M. Hewitt, Some genetic consequences of ice ages, and their role in divergence and speciation, Biol. J. Linn. Soc. 58 (1996) 247–276.
[3] G. Allegrucci, E. Trucchi, V. Sbordoni, Tempo and mode of species diversification in *Dolichopoda* cave crickets (Orthoptera, Rhaphidophoridae), Mol. Phylogenet. Evol. 60 (2011) 108–121.
[4] R.W. Bryson, L. PrendiniL, W.E. Savary, P.B. Pearman, Caves as microrefugia: Pleistocene phylogeography of the troglophilic North American scorpion *Pseudouroctonus reddelli*, BMC Evol. Biol. 14 (2014) 1–16.
[5] G.M. Hewitt, The genetic legacy of the Quaternary ice ages, Nature 405 (2000) 907–913.
[6] F. Ballarin, S.Q. Li, Diversification in tropics and subtropics following the mid-Miocene climate change: a case study of the spider genus *Nesticella*, Glob. Chang. Biol. 24 (2018) 577–591.
[7] Y. Zhang, S. Li, Ancient lineage, young troglobites: recent colonization of caves by *Nesticella* spiders, BMC Evol. Biol. 13 (2013) 183.
[8] C. Parmesan, G. Yohe, A globally coherent fingerprint of climate change impacts across natural systems, Nature 421 (2003) 37–42.
[9] M. Byrne, Evidence for multiple refugia at different time scales during Pleistocene climatic oscillations in southern Australia inferred from phylogeography, Quaternary Sci. Rev. 27 (2008) 2576–2585.
[10] D.B. Shepard, F.T. Burbrink, Phylogeographic and demographic effects of Pleistocene climatic fluctuations in a montane salamander, *Plethodon fourchensis*, Mol. Ecol. 18 (2009) 2243–2262.
[11] W.C. Funk, R.E. Lovich, P.A. Hohenlohe, C.A. Hofman, S.A. Morrison, T.S. Sillett, et al., Adaptive divergence despite strong genetic drift: genomic analysis of the evolutionary mechanisms causing genetic differentiation in the island fox (*Urocyon littoralis*), Mol. Ecol. 25 (2016) 2176–2194.
[12] R.C. Lacy, Loss of genetic diversity from managed populations: interacting effects of drift, mutation, immigration, selection, and population subdivision, Conserv. Biol. 1 (1987) 143–158.
[13] A.A. Hoffmann, C.M. Sgro, Climate change and evolutionary adaptation, Nature 470 (2011) 479–485.
[14] Y. Huang, X. Guo, S.Y.W. Ho, H. Shi, J. Li, J. Li, et al., Diversification and demography of the Oriental garden lizard (*Calotes versicolor*) on Hainan Island and the Adjacent Mainland, PLoS One 8 (2013), e64754.
[15] Y. Liu, C.H. Dietrich, C. Wei, Genetic divergence, population differentiation and phylogeography of the cicada *Subpsaltria yangi* based on molecular and acoustic data: an example of the early stage of speciation? BMC Evol. Biol. 19 (2019) 5.
[16] W. Zhao, M. Wang, Y. Liu, X. Gong, K. Dong, D. Zhou, S. He, Phylogeography of *Apis cerana* populations on Hainan island and southern mainland China revealed by microsatellite polymorphism and mitochondrial DNA, Apidologie 48 (2017) 63–74.
[17] Z. Li, G. Yu, D. Rao, J. Yang, Phylogeography and demographic history of *Babina pleuraden* (Anura, Ranidae) in southwestern China, PLoS One 7 (2012), e34013.
[18] M.P. Miller, M.R. Bellinger, E.D. Forsman, S.M. Haig, Effects of historical climate change, habitat connectivity, and vicariance on genetic structure and diversity across the range of the red tree vole (*Phenacomys longicaudus*) in the Pacific northwestern United States, Mol. Ecol. 15 (2006) 145–159.
[19] E. Eizirik, J.H. Kim, M. Menotti-Raymond, P.G. Crawshaw, S.J. O'Brien, W.E. Johnson, Phylogeography, population history and conservation genetics of jaguars (*Panthera onca*, Mammalia, Felidae), Mol. Ecol. 10 (2001) 65–79.
[20] G.M. Hewitt, Genetic consequences of climatic oscillations in the Quaternary, Philos. T. Roy. Soc. B. 359 (2004) 183–195.
[21] K. Lambeck, T.M. East, E.M. Potter, Links between climate and sea levels for the past three million years, Nature 419 (2002) 199–206.
[22] J.C. Avise, J. Arnold, R.M. Ball, E. Bermingham, T. Lamb, J.E. Neigel, et al., Intraspecific phylogeography: the mitochondrial DNA bridge between population genetics and systematics, Annu. Rev. Eco. Evol. S. 18 (1987) 489–522.
[23] F. Rodríguez-Sánchez, D. Gavin G., M. Fitzpatrick, P. Gugger F., K. Heath D., S. Dobrowski Z., et al., Climate refugia: joint inference from fossil records, species distribution models and phylogeography, New Phytol. 204 (2014) 37–54.
[24] R. Mellick, A. Lowe, C. Allen, R.S. Hill, M. Rossetto, Palaeodistribution modelling and genetic evidence highlight differential post-glacial range shifts of a rain forest conifer distributed across a latitudinal gradient, J. Biogeogr. 39 (2012) 2292–2302.
[25] F. Yan, W. Zhou, H. Zhao, Z. Yuan, Y. Wang, K. Jiang, et al., Geological events play a larger role than Pleistocene climatic fluctuations in driving the genetic structure of *Quasipaa boulengeri* (Anura: Dicroglossidae), Mol. Ecol. 22 (2013) 1120–1133.
[26] D.I. Axelrod, P.H. Al-ShehbazI, Raven, History of the modern flora of China, in: A.L. Zhang, S.G. Wu (Eds.), Floristic Characteristics and Diversity of East Asian Plants, Springer, New York, 1996.
[27] Y. Wang, W. Jiang, H. Comes, F. Hu, Y. Qiu, C. Fu, Molecular phylogeography and ecological niche modelling of a widespread herbaceous climber, *Tetrastigma hemsleyanum* (Vitaceae): insights into Plio-Pleistocene range dynamics of evergreen forest in subtropical China, New Phytol. 206 (2015) 852–867.
[28] N. Myers, R.A. Mittermeier, C.G. Mittermeier, G.A.B. da Fonseca, J. Kent, Biodiversity hotspots for conservation priorities, Nature 403 (2000) 853–858.
[29] J. Xue, X. Yu, H. Zhang, X. Chen, W. Bu, Population genetics and ecological niche modeling shed light on conservation of the island endemic damselfly *Pseudolestes mirabilis* (Odonata, Pseudolestidae), Hydrobiologia 790 (2017) 273–286.
[30] P.L.T. Beuk, Cicadas Spreading by Island or Spreading the Wings? Historic Biogeography of Dundubiine Cicadas of the Southeast Asian Continent and Archipelagos, Ph.D. thesis University of Amsterdam, 2002.
[31] D.C. Marshall, K.B. Hill, K.M. Fontaine, T.R. Buckley, C. Simon, Glacial refugia in a maritime temperate climate: cicada (*Kikihia subalpina*) mtDNA phylogeography in New Zealand, Mol. Ecol. 18 (2009) 1995–2009.
[32] K.B.R. Hill, C. Simon, D.C. Marshall, G.K. Chambers, Surviving glacial ages within the Biotic Gap: phylogeography of the New Zealand cicada *Maoricicada campbelli*, J. Biogeogr. 36 (2009) 675–692.
[33] G.A. Pinto-Juma, J.A. Quartau, M.W. Bruford, Population structure of *Cicada barbara* Stål (Hemiptera, Cicadoidea) from the Iberian Peninsula and Morocco based on mitochondrial DNA analysis, B. Entomol. Res. 98 (2008) 15–25.
[34] Y. Liu, Y. Qiu, X. Wang, H. Yang, H. Hayashi, C. Wei, Morphological variation, genetic differentiation and phylogeography of the East Asia cicada *Hyalessa maculaticollis* (Hemiptera: Cicadidae), Syst. Entomol. 43 (2018) 308–329.
[35] S. Osozawa, S. Shiyake, H. Fukuda, J. Wakabayashi, Quaternary vicariance of *Platypleura* (Hemiptera: Cicadidae) in Japan, Ryukyu, and Taiwan islands, Biol. J. Linn. Soc. 121 (2017) 185–199.
[36] R.A. Pyron, F.T. Burbrink, Hard and soft allopatry: physically and ecologically mediated modes of geographic speciation, J. Biogeogr. 37 (2010) 2005–2015.
[37] S. Ye, H. Huang, R. Zheng, J. Zhang, G. Yang, S. Xu, Phylogeographic analyses strongly suggest cryptic speciation in the giant spiny frog (Dicroglossidae: *Paa spinosa*) and interspecies hybridization in *Paa*, PLoS One 8 (2013), e70403.
[38] L. Shu, P. Deng, J. Yu, J. Yu, Y. Wang, S. Jiang, The age and tectonic environment of the rhyolitic rocks on the western side of Wuyi Mountain, South China, Sci. China Ser. D. 51 (2008) 1053–1063.
[39] Q. Zhu, B. Liao, P. Li, J. Li, X. Deng, X. Hu, X. Chen, Phylogeographic pattern suggests a general northeastward dispersal in the distribution of *Machilus pauhoi* in South China, PLoS One 12 (2017), e0184456.
[40] J. Wang, P. Gao, M. Kang, A.J. Lowe, H. Huang, Refugia within refugia: the case study of a canopy tree (*Eurycorymbus cavaleriei*) in subtropical China, J. Biogeogr. 36 (2009) 2156–2164.
[41] D. Chen, H. Kang, C. Liu, An overview on the potential quaternary glacial refugia of plants in China mainland, Bulletin Botani. Res. 31 (2011) 623–632.

[42] Z. Zhao, Is there Quaternary Glaciation in the Wuyi Mountain? Da Zi Ran, 4, 1981 14–16 (Chinese).
[43] S. Osozawa, N.V. Vuong, V.V. Tich, J. Wakabayashi, Reactivation of a collisional suture by Miocene transpressional domes associated with the Red River and Song Chay detachment faults, northern Vietnam, J. Asian Earth Sci. 1 (2015) 6.
[44] P. Tapponnier, R. Lacassin, P. Leloup, U. Scharer, Z. Dalai, W. Haiwei, et al., The Ailao Shan/Red River metamorphic belt: tertiary left-lateral shear between Indochina and South China, Nature 343 (1990) 431–437.
[45] Q. Yan, X. Shi, P.R. Castillo, The late mesozoic–cenozoic tectonic evolution of the South China Sea: a petrologic perspective, J. Asian Earth Sci. 85 (2014) 178–201.
[46] U. Barckhausen, M. Engels, D. Franke, S. Ladage, M. Pubellier, Evolution of the South China Sea: revised ages for breakup and seafloor spreading, Mar. Petrol. Geol. 58 (2014) 599–611.
[47] L.D. Gilley, T.M. Harrison, P.H. Leloup, F.J. Ryerson, O.M. Lovera, J.H. Wang, Direct dating of left-lateral deformation along the Red River shear zone, China and Vietnam, J. Geophys. Res: Sol. Ea. 108 (2003) 2127.
[48] P. Molnar Hallet, Distorted drainage basins as markers of crustal strain east of the Himalaya, J. Geophys. Res: Sol. Ear. 106 (B) (2001) 13697–13709.
[49] T. Phan Trong, L. Van Ngo, H. Van Nguyen, H.Q. Vinh, B. Van Thom, B.T. Thao, et al., Late Quaternary tectonics and seismotectonics along the Red River fault zone, North Vietnam, Earth-Sci. Rev. 114 (2012) 224–235.
[50] R.H. Bain, M.M. Hurley, A biogeographic synthesis of the amphibians and reptiles of Indochina, B. Am. Mus. Nat. Hist. 360 (2011) 1–138.
[51] I. Chou, Z. Lei, L. Li, X. Lu, W. Yao, The Cicadidae of China (Homoptera: Cicadoidea), Tianze Press, Hong Kong, 1997.
[52] H.T. Pham, T.H. Nguyen, H.Y.A. Luu, Checklist of the Cicadidae (Hemiptera: Auchenorrhyncha) from northern Vietnam. Tiêu Ban Khu Hệ Động Vật–Thực Vật, 2016 375.
[53] M.A.J. Williams, D.L. Dunkerley, P. De Deckker, A.P. Kershaw, J. Chappel, Quaternary Environments, Arnold, London, 1998.
[54] X. Jianga, E.M. Gardnerc, H. Meng, M. Deng, G. Xu, Land bridges in the Pleistocene contributed to flora assembly on the continental islands of South China: insights from the evolutionary history of *Quercus championii*, Mol. Phylogenet. Evol. 13 (2019) 236–245.
[55] H. Zhao, L. Wang, J. Yuan, Origin and time of Qiongzhou Strait, Mar. Geol. Quaternary Geol. 27 (2007) 33.
[56] Y.C. Chiang, K.H. Hung, B.A. Schaal, X.J. Ge, T.W. Hsu, T.Y. Chiang, Contrasting phylogeographical patterns between mainland and island taxa of the *Pinus luchuensis* complex, Mol. Ecol. 15 (2006) 765–779.
[57] S.L. Lee, K.K.S. Ng, L.G. Saw, A. Norwati, M.H. Siti Salwana, C.T. Lee, M. Norwati, Population genetics of *Intsia palembanica* (Leguminosae) and genetic conservation of virgin jungle reserves in peninsular Malaysia, Am. J. Bot. 89 (2002) 447–459.
[58] L.R. Nielsen, Molecular differentiation within and among island populations of the endemic plant *Scalesia affinis* (Asteraceae) from the Galápagos Islands, Heredity 93 (2004) 434–442.
[59] J. Dodson, J. Li, F. Lu, W. Zhang, H. Yan, S.A. Cao, Late Pleistocene and Holocene vegetation and environmental record from Shuangchi Maar, Hainan Province, South China. Palaeogeogr. Palaeocl. 523 (2019) 89–96.
[60] Z. Hu, A. Kantachumpoo, R. Liu, Z. Sun, J. Yao, T. Komatsu, et al., A late Pleistocene marine glacial refugium in the southwest of Hainan Island, China: Phylogeographical insights from the brown alga *Sargassum polycystum*, J. Biogeogr. 45 (2017) 355–366.
[61] R.J. Petit, C. Bodénès, A. Ducousso, G. Roussel, A. Kremer, Hybridization as a mechanism of invasion in oaks, New Phytol. 161 (2004) 151–164.
[62] S. Osozawa, R. Shinjo, A. Armid, Y. Watanabe, T. Horiguchi, J. Wakabayashi, Palaeogeographic reconstruction of the 1.55 Ma synchronous isolation of the Ryukyu Islands, Japan, and Taiwan and inflow of the Kuroshio warm current, Int. Geol. Rev. 54 (2012) 1369–1388.
[63] H.Y. Tseng, W.S. Huang, M.L. Jeng, R.J.T. Villanueva, O.M. Nuneza, C.P. Lin, Complex inter-island colonization and peripatric founder speciation promote diversification of flightless *Pachyrhynchus* weevils in the Taiwan–Luzon volcanic belt, J. Biogeogr. 45 (2018) 89–100.
[64] R. Nathan, Long-distance dispersal of plants, Science 313 (2006) 786–788.
[65] N.T. Thanh, P.J. Liu, M.D. Dong, D.H. Nhonet, D.H. Cuong, B.V. Dung, et al., Pleistocene-Holocene sequence stratigraphy of the subaqueous Red River delta and the adjacent shelf, Vietnam J. Earth Sci. 40 (2018) 271–287.
[66] Z. Hou, H. Zhong, C. Nansen, C. Wei, An integrated analysis of hyperspectral and morphological data of cicada ovipositors revealed unexplored links to specific oviposition hosts, Zoomorphology 138 (2019) 265–276.
[67] X. Zhang, Z. Wu, Z. Cao, Flora of China. 23, No 1, Science Press, Beijing, 1998 112–113.
[68] D. Zhang, Z. Ye, K. Yamada, Y. Zhen, C. Zheng, W.J. Bu, Pleistocene sea level fluctuation and host plant habitat requirement influenced the historical phylogeography of the invasive species *Amphiareus obscuriceps* (Hemiptera: Anthocoridae) in its native range, BMC Evol. Biol. 16 (2016) 174.
[69] H.K. Voris, Maps of Pleistocene sea levels in Southeast Asia: shorelines, river systems and time durations, J. Biogeogr. 27 (2000) 1153–1167.
[70] A.R. Rogers, H. Harpending, Population growth makes waves in the distribution of pairwise genetic differences, Mol. Biol. Evol. 9 (1992) 552–569.
[71] F. Wu, X. Fang, Y. Miao, M. Dong, Environmental indicators from comparison of sporopollen in early Pleistocene lacustrine sediments from different climatic zones, Chin. Sci. Bull. 55 (2010) 2981–2988.
[72] A. Favre, M. Päckert, S.U. Pauls, S.C. Jähnig, D. Uhl, I. Michalak, et al., The role of the uplift of the Qinghai-Tibetan plateau for the evolution of Tibetan biotas, Biol. Rev. 90 (2015) 236–253.
[73] T.M. Harrison, P. Copeland, W.S.F. Kidd, A. Yin, Raising Tibet, Science 255 (1992) 1663–1670.
[74] T. Schmitt, Molecular biogeography of Europe: Pleistocene cycles and postglacial trends, Front. Zool. 4 (2007) 11.
[75] A. Blach-Overgaard, J.C. Svenning, J. Dransfield, M. Greve, H. Balslev, Determinants of palm species distributions across Africa: the relative roles of climate, non-climatic environmental factors, and spatial constraints, Ecography 33 (2010) 380–391.
[76] D.W. Purves, J. Dushoff, Directed seed dispersal and metapopulation response to habitat loss and disturbance: application to *Eichhornia paniculata*, J. Ecol. 93 (2005) 658–669.
[77] J. Fischer, D. Lindenmayer, Landscape modification and habitat fragmentation: a synthesis, Glob. Ecol. Biogeogr. 16 (2007) 265–280.
[78] D. Tilman, J. Fargione, B. Wolff, C.D. Antonio, A. Dobson, R. Howarth, et al., Forecasting agriculturally driven global environmental change, Science 292 (2001) 281–284.
[79] J. Provan, K.D. Bennett, Phylogeographic insights into cryptic glacial refugia, Trends Ecol. Evol. 23 (2008) 564–571.
[80] L.M. Chan, J.L. Brown, A.D. Yoder, Integrating statistical genetic and geospatial methods brings new power to phylogeography, Mol. Phylogenet. Evol. 59 (2011) 523–537.
[81] H. Ren, X.A. Cai, C.H. Li, Y.S. Ye, Atlas on Tool Species of Vegetation Recovery in South China, Huazhong University of Science & Technology Press, Wuhan, 2010.
[82] C.H. Chen, Cicadas of Taiwan, Big Trees Publication, Taipei, Taiwan, 2004 (Chinese).
[83] R. Lanfear, B. Calcott, S.Y.W. Ho, S. Guindon, PARTITIONFINDER: combined selection of partitioning schemes and substitution models for phylogenetic analyses, Mol. Biol. Evol. 29 (2012) 1695–1701.
[84] D. Silvestro, I. Michalak, RaxmlGUI: a graphical front-end for RAxML, Org. Divers. Evol. 12 (2012) 335–337.
[85] J. Felsenstein, Confidence limits on phylogenies: an approach using the bootstrap, Evolution 39 (1985) 783–791.
[86] F. Ronquist, J.P. Huelsenbeck, MrBayes3: Bayesian phylogenetic inference under mixed models, Bioinformatics 19 (2003) 1572–1574.
[87] Rambaut A., Drummond A.J., Tracer Version1.5.0. Available at: http://beast.bio.ed.ac. uk/software/tracer/. (2009).
[88] P. Librado, J. Rozas, DnaSP v5: a software for comprehensive analysis of DNA polymorphism data, Bioinformatics 25 (2009) 1451–1452.
[89] D.H. Huson, D. Bryant, Application of phylogenetic networks in evolutionary studies, Mol. Biol. Evol. 23 (2006) 254–267.
[90] H.J. Bandel, P. Forster, A. Röhl, Median-joining networks for inferring intraspecific phylogenies, Mol. Biol. Evol. 16 (1999) 37–48.
[91] I. Dupanloup, S. Schneider, L. Excoffier, A simulated annealing approach to define the genetic structure of populations, Mol. Ecol. 11 (2002) 2571–2581.
[92] L. Excoffier, P.E. Smouse, J.M. Quattro, Analysis of molecular variance inferred from metric distances among DNA haplotypes: application to human mitochondria DNA restriction sites, Genetics 131 (1992) 479–491.
[93] L. Excoffier, H.E. Lischer, Arlequin suite ver 3.5: a new series of programs to perform population genetics analyses under Linux and Windows, Mol. Ecol. Resour. 10 (2010) 564–567.
[94] E. Bonnet, D. Van, Y. Peer, ZT: a software tool for simple and partial Mantel tests, J. Stat. Softw. 7 (2002) 1–12.
[95] J.K. Pritchard, X. Wen, D. Falush, Documentation for Structure Software: Version 2.3, Available at http://pritch.bsd.uchicago.edu/structure 2009.
[96] M. Hubisz, D. Falush, M. Stephens, J. Pritchard, Inferring weak population structure with the assistance of sample group information, Molr. Ecol. Resour. 9 (2009) 1322–1332.
[97] J.K. Pritchard, M. Stephens, P. Donnelly, Inference of population structure using multilocus genotype data, Genetics 155 (2000) 945–959.
[98] G. Evanno, S. Regnaut, J. Goudet, Detecting the number of clusters of individuals using the software STRUCTURE: a simulation study, Mol. Ecol. 14 (2005) 2611–2620.
[99] D.A. Earl, B.M. von Holdt, STRUCTURE HARVESTER: a website and program for visualizing STRUCTURE output and implementing the Evanno method, Conserv. Genet. Resour. 4 (2012) 359–361.
[100] M. Jakobsson, N.A. Rosenberg, CLUMPP: a cluster matching and permutation program for dealing with label switching and multimodality in analysis of population structure, Bioinformatics 23 (2007) 1801–1806.
[101] N.A. Rosenberg, DISTRUCT: a program for the graphical display of population structure, Mol. Ecol. Notes 4 (2004) 137–138.
[102] A.J. Drummond, M.A. Suchard, D. Xie, A. Rambaut, Bayesian phylogenetics with BEAUti and the BEAST 1.7, Mol. Biol. Evol. 29 (2012) 1969–1973.
[103] A.J. Drummond, A. Rambaut, BEAST: Bayesian evolutionary analysis by sampling trees, BMC Evol. Biol. 7 (2007) 214.
[104] A. Rambaut, Figtree, a Graphical Viewer of Phylogenetic Trees, Retrieved from http://tree.bio.ed.ac.uk/software/gtree 2016.
[105] C.L. Owen, D.C. Marshall, K.B. Hill, C. Simon, How the aridification of Australia structured the biogeography and influenced the diversification of a large lineage of Australian cicadas, Syst. Biol. 66 (2016) 1–21.
[106] J. Heled, A.J. Drummond, Bayesian inference of species trees from multilocus data, Mol. Biol. Evol. 27 (2010) 570–580.
[107] A.V.Z. Brower, Rapid morphological radiation and convergence among races of the butterfly *Heliconius erato* inferred from patterns of mitochondrial DNA evolution, Proc. Nati. Acad. Sci. U. S. A. 91 (1994) 6491–6495.
[108] A.J. Drummond, A. Rambaut, B. Shapiro, O. Pybus, Bayesian coalescent inference of past population dynamics from molecular sequences, Mol. Biol. Evol. 22 (2005) 1185–1192.

[109] Y. Yu, A.J. Harris, X.J. He, RASP (Reconstruct Ancestral State in Phylogenies) 3.0, http://mnh.scu.edu.cn/soft/blog/RASP 2015.
[110] J.A. Nylander, U. Olsson, P. Alström, I. Sanmartín, Accounting for phylogenetic uncertainty in biogeography: a Bayesian approach to dispersal-vicariance analysis of the thrushes (Aves: *Turdus*), Syst. Biol. 57 (2008) 257–268.
[111] I. Sanmartín, P. Van Der Mark, F. Ronquist, Infer-ring dispersal: a Bayesian approach to phylogeny-based island biogeography, with special reference to the Canary Islands, J. Biogeogr. 35 (2008) 428–449.
[112] Maddison W.P., Maddison D.R., Mesquite: A Modular System for Evolutionary Analysis. Version 3.04. URL http://mesquiteproject.org. (2015).
[113] E. Paradis, J. Claude, K. Strimmer, APE: analyses of phylogenetics and evolution in R language, Bioinformatics 20 (2004) 289–290.